1

Overview of Nonlinear Optics

Elsa Garmire
Dartmouth College,
USA

1. Introduction

The invention of the laser provided enough light intensity that nonlinear optics (NLO) could be observed for the first time, almost exactly one year after the first ruby laser – second harmonic generation, observed fifty years ago (Franken, 1961), with a theoretical examination of interactions between light waves in a nonlinear dielectric following very soon thereafter (Armstrong, 1962). The field has grown so enormously that it is impossible to review all topics. Theoretical approaches have bifurcated into macroscopic and microscopic viewpoints. Both have validity and usefulness, but this review will focus primarily on experimental results and applications, as well as models for optical nonlinearities that stress the macroscopic character of materials, with parameters determined experimentally. At times the wavelike nature of light is sufficient to explain concepts and at other times it is easier to refer to the photon-like nature of light. In nonlinear optics we become fluent in both concepts.

Table 1 shows a classification scheme that tries to put some order into the many phenomena that comprise nonlinear optics. Optical nonlinearities occur when the output of a material or device ceases to be a linear function of the input power, which is almost always the case for high enough intensities. The nonlinearity may cause a light-induced change in refractive index or absorption of the medium or it may cause new frequencies to be generated.

Character of medium:	Transparent	Absorbing	Scattering	Non-Local	
Atom-light interaction:	Non-resonant	Resonant	Incoherent	Coherent	Transient
Optics geometry:	Plane Wave	Finite Beam	Waveguide	Wave-Mixing	Reflection
Device Geometries:	Bulk	Periodic	Fibers	Resonators	Micro-cavities

Table 1. Classification of nonlinear optical phenomena

1.1 Character of the medium

The character of the dielectric medium may be such that it is transparent, absorbing or scattering to the incident light. Usually the medium responds to the local optical intensity;

however, in some cases the nonlinearity is non-local, so that light intensity at one point creates a change in absorption or refractive index at another point. Examples of non-local nonlinearities are absorptive thermal effects and optically-induced carrier-transport, such as occurs in photo-refractivity.

1.2 Atom-light interaction

When its frequency does not match any atomic or molecular resonance, low intensity light is transmitted through transparent media without loss; this non-resonant interaction with the medium is expressed as a refractive index. At higher intensities, the nonlinearity is due to a nonlinear refractive index. Stimulated scattering such as Stimulated Raman Scattering (SRS), and Stimulated Brillouin Scattering (SBS) phenomena represent another class of non-resonant nonlinearities.

When its frequency is resonant with atomic or molecular transitions, light is absorbed, with a magnitude expressed in terms of an absorption coefficient. At high intensity, saturable absorption may occur, due to filling the available upper states. In this case the absorption begins to decrease with intensity and the material may become transparent. Even if the medium is initially transparent, when the incident light is sufficiently intense, multi-photon absorption may take place, as a result of near-resonance between the medium's absorption lines and multiples of the incident light frequency. Multi-photon absorption causes an increasingly large absorption as the light intensity increases.

Typically individual atoms or molecules lose their coherence during their interaction with light, so that the light-matter effects can be understood as incoherent phenomena. However, with sufficiently short pulses, or long coherence times, nonlinear phenomena will demonstrate coherent interactions between the light and the medium, in which phase is preserved. Examples are self-induced transparency and pi pulses. A number of transient phenomena do not require phase coherence – an example is self-phase modulation.

Nonlinear optics occurs when any of these interactions are changed by the intensity of the incident light, thereby affecting the output. Some authors consider "nonlinear optics" to be any phenomenon that changes the way light interacts with a medium, such as by changing the refractive index through applying an external voltage (e.g. electro-optical modulators). This chapter does *not* consider these effects. The formal definition of nonlinear optics used here requires that the light itself must cause the material properties to change and thereby change how it interacts with light (either the initial lightwave or another lightwave).

In almost all of its manifestations, nonlinear optics can be explained classically – quantum mechanics is not usually required. Most of the nonlinear effects can be explained by a macroscopic view of the medium through a nonlinear polarization and/or nonlinear absorption coefficient. In some cases it is more useful to consider how the microscopic behavior of individual molecules adds up to result in nonlinear phenomenon – this is particularly true with resonant interactions.

1.3 Optics geometries

Many optical nonlinearities use a broad beam of light incident on a nonlinear medium, which is modeled as a plane wave. Direct observation of harmonics generated from a plane

wave can occur as long as there is *phase-matching*. Direct observation of nonlinear absorption is made through intensity measurements. The nonlinear refractive index is often observed through changes in the spatial profile of a beam of finite width, which is most dramatic with self-focusing or thermal blooming and is described in the Z-scan discussion in section 2.

Because diffraction from a finite beam shortens the length over which the nonlinearity is large, waveguides are often used in nonlinear optics geometries. If the phase-matching condition is met, the beam can be focused into a waveguide and won't spread out; the nonlinear interaction can remain large over rather long lengths.

Wave-mixing describes the fact that two plane waves overlapping within a nonlinear medium can mix the waves together in a nonlinear way. This may occur from nonlinear refractive index and/or nonlinear absorption. The nonlinearity introduces a periodicity in the medium due to these mixing waves that refracts additional waves. The result is a nonlinear diffracting grating. There can be two-wave mixing, three-wave mixing or four-wave mixing. Measuring the nonlinear refractive index by interfering a beam with a reference beam through a nonlinear medium represents another kind of wave-mixing.

Finally, optical nonlinearities can occur in reflection from a nonlinear interface, which can be demonstrated using prism coupling. Surfaces can enhance optical nonlinearities, particularly in micro-cavities.

1.4 Device geometries

All of the nonlinear processes described above can be used in a variety of device geometries. Descriptions generally begin with bulk media, but can be replaced by periodic media that can be quasi-phase-matched, or that provide reflective gratings. Fibers have the advantage of producing intense light in waveguides of very small cores over very long distances. While the glass fibers usually have small nonlinearities, most nonlinear phenomena can build up to be quite large in fibers because of their very long length.

Optical resonators can enhance the optical cavity field, effectively enlarging the optical nonlinearities. An example is the intra-cavity frequency-doubled diode-pumped solid-state laser used today as the ubiquitous green laser pointer. The Fabry-Perot etalon was shown to demonstrate optical bistability, when filled with a nonlinear refractive index and/or absorpting material. Another form of optical resonator is the micro-sphere (even quantum dots), which have exhibited enhanced optical fields and therefore enhanced nonlinearities. Closely related, but not detailed here, are enhanced nonlinearities due to surface polaritons at metal-dielectric surfaces.

1.5 NLO and its applications

Nonlinear optics is a very broad field, centered in both Physics and Electrical Engineering, more specifically in the sub-fields of Optics and Photonics. Select the topic "nonlinear optics" in the ISI Web of Science and I found 7,240 papers in September, 2011. Google found 910,000 pages on the same day! It is interesting that the 50 most cited papers were published in 26 different journals! This is because nonlinear optics impacts a wide range of technical fields, including optical communications, fiber optics, ultrafast lasers, quantum computing, ultra-cold atoms, plasma physics, particle accelerators, etc. Both chemistry and biology are using increasing amounts of nonlinear optics. Nonlinear optics applies to numerous specific

applications, such as in fiber optics, spectroscopy, photorefractivity, liquid crystals, polymers, semiconductors, organics, switching, ultraviolet, X-rays, quantum optics, telecommunications and signal processing. This review will not explore applications in detail, only introduce a few of the most important. A great deal of information about nonlinear optics is now available on the web.[1]

This chapter will introduce the important basic phenomena of nonlinear optics and their applications, along with some of the most important concepts. Macroscopic, classical concepts will be emphasized, although simple quantum mechanics concepts can be introduced in a straight-forward manner.

2. Nonlinear polarization density

The origin of nonlinear optics is the nonlinear response of the material to internal electric fields. The material response is manifest in a *susceptibility*. The linear susceptibility is related to the refractive index through $\chi_1 = n^2 - 1$. When intense light enters a transparent material, its susceptibility can become nonlinear. It is usually sufficient to consider this heuristically as a Taylor expansion in the electric field:

$$\chi(E) = \chi_1 + \chi_2 E + \chi_3 E^2 + \chi_4 E^3 \ldots \quad (1)$$

All higher orders beyond χ_1 represent the nonlinear response of a material to the presence of intense light. The higher order terms fall off in magnitude very rapidly unless the light intensity is very high. In general the susceptibility is a tensor and the vector component of the fields must be taken into account.

The effect of the susceptibility on the light traveling through the medium is manifest in the *polarization density,* **P.** In tensor notation the linear polarization is $\mathbf{P} = \varepsilon_0 \chi_1 : \mathbf{E}$. The nonlinear polarization density is $\mathbf{P}_{NL} = \varepsilon_o \chi(\mathbf{E}) : \mathbf{E}$, so the second order polarization is $\mathbf{P}_2 = \varepsilon_0 \chi_2 : \mathbf{EE}$ and the third-order nonlinear polarization is $\mathbf{P_3} = \varepsilon_0 \chi_3 : \mathbf{EEE}$. There is no universal notation, however; the nonlinear refractive index (a third-order nonlinearity) is often written in terms of intensity as $n(I) = n_o + n_2 I$. Thus the nonlinear component of the refractive index that is linear in intensity is called n_2, while the related susceptibility is χ_3.

2.1 Second-order nonlinear polarization density, P_2.

For two incident waves, one at frequency ω_o, and the other at ω_1, the nonlinear term χ_2 will introduce (ignoring tensor notation) $P_2 = \chi_2 E_o \cos(\omega_o t - k_o z) E_1 \cos(\omega_1 t - k_1 z)]$, where amplitudes are E_o and E_1 and wave vectors k_o and k_1 are related to frequencies by their respective velocities of light. This product gives two polarization terms, one that oscillates at $\omega_o + \omega_1$, and the other at $\omega_o - \omega_1$. Both terms are proportional to the product of the fields. From the quantum mechanical point of view, the nonlinearity has induced two photons to combine into one photon. When the two photons have the same frequency, one term yields *second*

[1] Wikipedia is quite reliable for investigating the phenomena outlined in this paper. Almost any of the topics discussed in this paper will be found in Wikipedia. See also, "An Open Access Encyclopedia for Photonics and Laser Technology," written by Dr. Rüdiger Paschotta, a consultant in photonics, http://www.rp-photonics.com/topics_nonlinear.html, which covers the basics of nonlinear optics rather well, with good search capability.

harmonic and the other yields a term with a *static field* (the frequency dependence cancels out). When the incident photons are different, *sum* and *difference* frequency photons are generated. An important criterion for materials to exhibit a susceptibility linear in the field, X_2E, is that they contain no center of inversion symmetry. Liquids, gases, amorphous solids and crystalline materials with high symmetry will not directly generate second harmonic. Typically the goal of X_2E terms is to transfer power from one frequency to another, while maintaining a coherent beam. This requires *phase-matching*, which will be discussed later.

2.1.1 Second Harmonic Generation (SHG)

Perhaps the most important application of P_2 is converting infrared light into visible. The green laser pointer consists of a diode-pumped solid state laser emitting in the infrared at 1.06 μm that is frequency-doubled by a nonlinear crystal to a wavelength of 0.53 nm. For one incident wave of frequency ω_o, the nonlinear term χ_2 introduces into the polarization P_2 a term that oscillates at $2\omega_o$, the second harmonic. Applications for SHG go considerably beyond laser pointers. Lasers that directly emit visible light are less efficient than infrared lasers, so when visible light is required, it is preferable to start with the more efficient infrared lasers and to frequency-double them. SHG has been a standard complement for Nd:YAG lasers for a long time. Diode-pumping has replaced lamp-pumping for most of these applications, increasing their efficiency. Visible (or ultra-violet) lasers are commonly used to pump other lasers, most notably the titanium-sapphire laser (and formerly, the dye laser). The highly inefficient argon laser is rapidly being replaced by frequency-doubled diode-pumped solid state lasers for applications such as pumping the ultra-short pulse titanium-sapphire lasers, which can be mode-locked to pulses only a few femtoseconds long and emit at 800-900 nm wavelengths.

How are these femtosecond pulses measured? With an *autocorrelator* that measures the physical length of fs pulses by means of SHG. An autocorrelator is created by splitting an ultra-short pulse train into two beams, and colliding them in a SHG crystal in such as way that the harmonic occurs only when both pulses overlap (a particular crystal geometry). Delaying one beam with respect to the other, and scanning this delay, enables the length of the pulse in physical space to be determined. Without SHG, the entire field of ultra-fast optics would be severely hampered.

In addition to simply offering light you can see, SHG is important because each visible or UV photon has enough energy to cause a chemical reaction. In non-homogenous materials, the generation of second harmonic may select for specific regions. Examples range from separating out collagen and microtubules in live tissue (Zipfel, 2003) to observing coupled magnetic and electric domains in ferroelectromagnets (Fiebig, 2003). Surface science is an important application because the surface breaks the symmetry of the bulk and enables SHG that depends critically on the character of the surface. The surface can also offer resonance enhancement of the signal (Hsu, 2011); monolayer adsorption can be detected, for example of tin on GaAs (Shen, 1994; Mitchell, 2009). In other applications, surface SHG can monitor laser melting and separate amorphous from crystalline growth. As a spectroscopic tool, SHG has been used in a plethora of applications, such as probing surface states of metals, surface magnetization, and, using ultrashort pulses, a wide range ultrafast surface reactions and surface dynamics.

2.1.2 Sum and Difference Frequency Generation (SFG and DFG)

When the incident field E contains two frequencies ω_o and ω_i, sum frequency and/or difference frequency generation is possible, as seen directly from Eq. (1); the cross-term gives a polarization of the form $P_2 = \chi_2 E_o E_i$. SFG can convert infrared light at frequency ω_i into a visible signal at frequency $\omega_s = \omega_o + \omega_i$. When light at frequency ω_o is very intense, there is even an effective amplification of the weak infrared signal. SFG is one way to provide coherent UV light from visible light. If one of the visible lasers has a tunable frequency, the UV light's frequency can be tuned.

DFG has been used to create infrared light from two higher frequency laser beams. The term DFG usually refers to the case where the beams at the two incident frequencies have comparable intensity. The output infrared signal will be at $\omega_s = \omega_o - \omega_i$. When one beam is very intense and the other is weak, amplification will occur (as with SHG). This is often called *parametric amplification*, which will be described later.

DFG has applications in telecommunications, where Wavelength Division Multiplexing (WDM) puts many wavelengths on the same optical fiber. In real WDM systems, a way is needed to convert from one wavelength to another. DFG is attractive in several respects: it is an instantaneous process that can simultaneously convert up and down multiple channels with equal efficiencies, has negligible spontaneous emission noise and no intrinsic frequency chirp (Yoo, 1996; Yu, 2007).

2.1.3 Nonlinear Optical Rectification (NOR)

The nonlinear term corresponding to $P_r = \varepsilon_o \chi_2 EE^*$ has no time dependence, other than that of the magnitude of E. It creates a DC static polarization through the time-average of E^2. This process is traditionally called *optical rectification*. The major practical application of optical rectification has been the generation of Terahertz radiation through optical rectification of femtosecond pulses (Dragoman, 2004; Fueloep, 2011). Because of the time-dependence of these fs pulses, the "static" field is not time-independent, but rises and falls within the width of the fs pulse, generating broadband electromagnetic pulses in free space. This results in fields with variation at Terahertz frequencies waves that have sub-mm wavelengths. Coherent light in the THz frequency domain is rather new and applications are presently being developed, predominantly spectroscopy. For optical rectification, the χ_2 materials ZnTe and GaAs are typically used.

Other applications for NOR include accelerating electrons within a small distance by means of static field enhancement due to surface plasmons. This enhancement may provide nanoscale geometries for high-energy electron sources, where electrons are accelerated in the electric field of surface plasmons (Lenner, 2011). Just as SHG is sensitive to surface conditions, so is NOR. It has become an important technique for investigating semiconductor heterostructures and nanostructures, such as asymmetric quantum wells (Wang, 2009). Optical rectification has even enabled miniature silicon waveguides to detect light within the bandgap that would not normally be detected (Baehr-Jones, 2005).

One of the most exciting applications of NOR comes in "wakefield generation," which is a relativistic version of optical rectification that introduces longitudinal field effects that can be as large as transverse effects. Electromagnetic field intensities in excess of 10^{18} W/cm^2 lead

to relativistic electron motion in the laser field. In addition to NOR, other effects may occur, including relativistic focusing, relativistic transparency, nonlinear modulation and multiple harmonic generation, and strong coupling to matter and other fields (such as high-frequency radiation) (Mourou, 2006). Optics in the relativistic regime is an exciting new direction for nonlinear optics (Tsaur, 2011).

2.2 Phase-matching

Efficient growth of second harmonic, sum, or difference frequency requires the nonlinear polarization P_2 to remain in the same relative phase with the incident light over the entire interaction length. This is called *phase-matching*, with the phases of the incident and resultant waves remaining in synchronism. Lack of synchronism comes about because the refractive index is a function of wavelength (dispersion), with shorter wavelengths (the harmonics) typically having higher refractive indices than the fundamental. Phase coherence requires $(n_{2\omega} - n_{\omega})L < \lambda/4$, which may typically be tens of micrometers. But in SHG the path length required to build up substantial signal is usually the order of centimeters. Thus special techniques are required to match phases, including anisotropic crystals, periodic domain reversal (quasi-phase matching) and waveguides (matching dispersion or using Cerenkov output).

2.2.1 Phase-matching in anisotropic crystals

In *anisotropic crystals* the refractive index depends on the direction of the light's polarization and its propagation direction with respect to the crystal. This dependence enables nonlinear crystals cut in particular geometries to have their fundamental and second harmonic with the same phase velocity. This is the only way that phase-match can be achieved in uniform bulk crystals. Anisotropic crystal phase matching can be very sensitive to crystal angle and temperature; calculations of suitable angles require complicated tensor calculations, but fortunately the commercial venders know how to do this and sell crystals cut to the proper orientation. In *type I phase matching* the fundamental has a single linear polarization and the harmonic has a polarization perpendicular to the fundamental. These crystals can be tuned by changing temperature or by changing the angle, or both. *Type II phase matching* requires that the nonlinear process mix laser beams with orthogonal polarizations. The harmonic can be along either polarization. Critical phase matching uses the angular dependence of the refractive index with beams propagating off-axis to match polarizations, while non-critical phase matching heats the crystal to achieve phase- matching for beams that propagate along the axis (Paschotta, 2011).

Efficient harmonic generation requires highly nonlinear crystals; a great deal of research has gone into finding and growing suitable material. Originally only crystal quartz and potassium di-hydrogen phosphate (KDP) were available. Lithium niobate was the first of many crystals grown for the purpose of harmonic generation; now a plethora of crystals are available, depending on the particular application and wavelength.

Sum and difference frequency generation is calculated through the coupling between three waves, rather than two, but phase-matching is required for these processes, just as for second harmonic generation.

No one crystal is ideal. Phosphates provide the largest nonlinear crystals: KDP (potassium dihydrogen phosphate), KD*P (deuterated potassium dihydrogen phosphate) and ADP

(ammonium dihydrogen phosphate) are all grown in water-solution to very large size, and are quite impervious to optical damage, although hygroscopic. KDP is being grown in tremendous sizes for the inertial confinement fusion laser at Livermore Laboratories in California. The phosphates have transparency to below 200 nm and out to 2 μm, but their nonlinear coefficient is quite small: d_{eff} ~ 0.4 pm/V (pm = picometers = 10^{-12}m). By comparison, KTP (potassium titanyl phosphate) and KTA (potassium titanyl arsenate) have an order of magnitude higher nonlinearity: d_{eff} ~ 4 pm/V and are non-hygroscopic, but they are hard to grow and only small crystals are available. KTP is commonly used today to frequency-double diode-pumped solid state lasers. However, if the optical power becomes too high, KTP shows photo-induced "gray-tracks."

Lithium niobate has large nonlinearities with a transparency range from 420 nm out to 5.2 μm and a very high nonlinearity (d_{eff} = 5.8 pm/V) but exhibits debilitating photo-refractive effects (see later) unless heated or doped with oxides. Magnesium oxide doping is commonly used. Zinc oxide doping increases the nonlinearity to 16 pm/V and has better optical quality and lower absorption, but is limited to 250 MW/cm² of light intensity. Eighty times improvement in damage threshold is obtained with zirconium oxide doping, at the expense of roughly half the nonlinearity. Lithium Tantalate ($LiTaO_3$) has less optical damage than LN and doesn't require doping, but its nonlinearity is half that of LN. Potassium niobate ($KNbO_3$) has high nonlinearity and high damage threshold, which sounds ideal, but it has only a small temperature range of phase-matching, and, more importantly, shaking or stressing the crystal can cause domain changes, so it must be handled "smoothly," limiting its use.

Borates form another class of nonlinear crystals, transparent into the UV, with a high threshold to optical damage, but with considerably lower nonlinearity: LBO (lithium triborate) is transparent to 150 nm, but d_{eff} ~ 0.8 pm/V, roughly twice KDP. BBO (beta-barium borate) has a more respectable d_{eff} ~ 2 pm/V. Bismuth Borate (BiBO) has d_{eff} ~ 3.3 pm/V and the highest damage threshold. These crystals are excellent for high-power applications: they're inert to moisture, with a large acceptance angle and small walk-off angle and suitable for temperature-controllable non-critical phase-matching.

Research is underway on organic crystals for frequency doubling, but they have not yet proven more reliable than the above-mentioned crystals.

In the infrared, a different set of crystals has been developed, with higher nonlinearities but much lower damage thresholds. These include AGS ($AgGaS_2$) , transparent over 0.5 - 13 μm; AGSe ($AgGaSe_2$) transparent over 0.7 - 18 μm; also HGS ($HgGa_2S_4$) and $ZnGeP_2$. Gallium selenide (GaSe) has the record nonlinearitiy, d_{eff} = 70 pm/V and doubles out to 13 μm wavelength.

The crystals just discussed are anisotropic, required for birefringent phase matching. Periodic poling can provide quasi-phase matching, which removes the need for birefringence. It can also increase the nonlinearity in birefringent crystals; periodic poling of lithium niobate (PPLN) exhibits the effective nonlinear coefficient 4.5 times relative to homogeneous LN.

2.2.2 Quasi-Phase Matching (QPM)

In quasi-phase matching, the nonlinear coefficient is reversed every coherence length (coherence length L_c is the length over which the accumulated phase mismatch = π). Quasi-

phase matching is important when birefringent phase-matching is difficult; the crystal need not even be birefringent. Without QPM, the fundamental and harmonic would get out of phase after a distance L_c given by $(k_2 - 2k_1)L = \pm\pi$. If the optical axis is flipped periodically at this distance, the nonlinearity reverses sign and harmonic conversion can continue to build up. Although quasi-phase matching was suggested in the early days of NLO, it did not become practical until the invention of periodic poling (Byer, 1997).

Periodic poling engineers the ferroelectric domains within lithium niobate and similar nonlinear crystals. A strong electric field is applied via patterned electrodes on the crystal surface. Domain reversal occurs at field strengths above the coercive level, which can be anywhere from 2 - 21 kV/mm in LN, depending on the crystal characteristics. The period of the electrode pattern determines the wavelengths for which QPM will occur. This process works best for waveguides and samples less than 0.5 mm thick; it works best in the infrared, where electrode periods can be 10 μm or more. The most common materials that are periodically poled are MgO-doped lithium niobate (called PPLN), lithium tantalate and KTP, while PP potassium niobate has also been reported. Organic nonlinearities such as nonlinear polymers can be poled for QPM (Hung, 2008). Quasi-phase matching has also been reported in glasses and fibers. Its most practical application is often in waveguides.

Periodic poling has extended SHG from anisotropic crystals to polymers and semiconductors. In addition to spatially periodic poling by pulsed electric fields that creates domains with flipped crystal axes, electron bombardment and thermal pulsing have also been successful with QPM. Because of poling enhancement of X_2, harmonic output in PPLN can be many times what would be observed in a single crystal, for the same intensity (Parameswaran, 2002). Second-harmonic generation, difference-frequency generation, and optical parametric oscillation all have used QPM.

2.2.3 Phase-matching in waveguides

The first reason to use waveguides for SHG is that the intensity of the incident light can be maintained over a long length. Before QPM, it was necessary to match the phases of the guided fundamental wave with the guided harmonic. This ability was demonstrated by choosing a wavelength that matched the phases of an incident TM_0 fundamental and the TE_1 mode of its harmonic (Sohler, 1978). Phase-matching in waveguides requires an ability to tailor the guide's effective refractive index. With proper design, the fundamental can create a harmonic in a mode whose effective refractive index will match that of the fundamental, so that waveguide dispersion cancels the material dispersion. The two modes must also have sufficient overlap that a strong harmonic can build up. Some examples have been nonlinear Langmuir-Blodgett films (Penner, 1994), corona-poled sputtered glass films (Okada, 1992), dye polymers (Sugihara, 1991) and complex semiconductor waveguide structures (Abolghasem, 2009; Fiore, 1998; Malis, 2004). To date these techniques have not been reliable enough to be used in practical systems. Often coupling into waveguides is not easy; bulk SHG crystals are in much greater demand. By the year 2000 SHG in waveguides usually has incorporated quasi-phase-matching.

A different approach uses photonic crystal waveguides, which can be tuned to achieve phase-matching for SHG (Martorell, 1997; Broderick, 2000; Mondia, 2003; Torres 2004).

For completeness we mention SHG observed as a Cerenkov-phase-matched harmonic from a waveguide's fundamental mode. The harmonic wave has a phase velocity beyond cutoff

for the waveguide, so that it propagates freely in the substrate material, acting as the source of the observed Cerenkov radiation. This phase-matching technique creates a beam at a small angle to the waveguide and has been observed in lithium niobate (Li, 1990; Wang, 1995) as well as nonlinear photonic crystal waveguides (Zhang, 2008). Cerenkov SHG can be important in applications where guided SHG is not desired.

2.3 Theory of second harmonic generation

When there is negligible depletion of the fundamental, the amount of second harmonic is conveniently solved through the coupled mode equations. These equations demonstrate the coupling between the fundamental and its harmonic through the nonlinear susceptibility χ_2. Using complex notation, the polarization density vector introduced by interaction between two input fields is $P_k(\omega_3) = \sum_{ij} \varepsilon_o(\chi_{ijk}/2)E_i(\omega_1)^*E_j(\omega_2)$, where it is important to acknowledge the tensor character of χ_{ijk} For second harmonic, $\omega_1 = \omega_2$ and usually the direction i and j are parallel, so $E_i = E_j$. For any particular configuration of input fields, the summation over all relevant values of χ can be represented by $P_3(2\omega) = d_{eff}\varepsilon_o E(\omega)^2$. By convention the second harmonic coefficient d_{eff} is most often used as the nonlinear parameter; it is the effective magnitude of the tensor $d_{ijk} = \chi_{ijk}/2$, which depends on the specific configuration of the optical fields.

In lossless materials, the fundamental field E_ω and its harmonic $E_{2\omega}$ can be related by the following coupled mode equations:

Fundamental:

$$\partial E_\omega/\partial z = i\,(k_o/n_\omega)E_\omega^{*}\,E_{2\omega}\,d_{eff}\exp(i\Delta kz)$$

and Harmonic:

$$\partial E_{2\omega}/\partial z = i\,(k_o/n_{2\omega})\,d_{eff}\,E_\omega^{2}\exp(-i\Delta kz)$$

where Δk is the mismatch of wave-vectors: $\Delta k = 2k_\omega - 2k_{2\omega} = (n_\omega - n_{2\omega})2\omega/c = (n_\omega - n_{2\omega})4\pi/\lambda_o$ and d_{eff} is the effective nonlinear coefficien and λ_o is the free-space wavelength of the fundamental. Solving such equations demonstrates that power couples from the incident wave to its harmonic and then back again along the path length. Power couples into the harmonic for a length $(\Delta k/2)L_c = \pi$ and then begins to couple back again, so $L_c = \lambda_o/[2(n_o - n_1)]$. Numbers for L_c can vary considerably, from less than ten microns to 100 microns or more. In quasi-phase matching periodic poling compensates every time the two waves reach a distance L_c. Solving the coupled mode equation yields the intensity at the second harmonic $I(2\omega)$ in terms of the intensity at the fundamental, $I(\omega)$ as a function of sample length *l*:

$$I(2\omega, l) = \frac{2\omega^2 d_{\text{eff}}^2 l^2}{n_{2\omega} n_\omega^2 c^3 \epsilon_0}\left(\frac{\sin(\Delta kl/2)}{\Delta kl/2}\right)^2 I^2(\omega)$$

where

$$I(2\omega,l) << I.$$

This is the familiar sinc^2 function; for a given crystal length *l* and intensity I, the maximum harmonic intensity falls off as the phase mismatch grows.

When phase-matched (Δk = 0), the harmonic intensity will grow quadratically with the fundamental intensity and quadratically with distance l, until the fundamental begins to deplete. It is then necessary to include depletion of the fundamental into the calculations. In the case of exact match, the solution is quite simple:

$$I(2\omega, l) = I(\omega,0)\tanh^2\left(\frac{E_0 \omega d_{\text{eff}} l}{n_\omega c}\right)$$

In the large conversion limit, tanh → 1 and the second harmonic intensity becomes 1; the fundamental will be completely converted to harmonic as expected by energy conservation (half the number of photons, but twice the frequency for each).

3. The P_3 term

The third order term produces a polarization proportional to third order in the electric field: $P_3 = \varepsilon_o(\chi_3 E^2)E$. This leads to a polarization oscillating at the third harmonic, and also to a term in which the factor $(\chi_3 E^2)$ has no oscillation frequency; this term oscillates at the fundamental frequency of the incident light. Thus the third-order nonlinearity causes both third harmonic generation (THG) and also an intensity-dependent change in the refractive index, which becomes nonlinear, n(I). The third-order term does not require a material with a center of inversion symmetry; all materials have χ_3 terms.

3.1 Third and higher-order harmonics

Third-order nonlinearities arise from expanding the nonlinear susceptibility to third order in the electric field. The extension from second- to third- harmonic is relatively straightforward, at least in concept. Now there are three electric fields: E_o oscillating at ω_o, E_2 oscillating at ω_2 and E_3 oscillating at ω_3. Depending on the medium, third harmonic can be considered as being generated by three fundamental photons (requiring phase-matching) or by a single incident photon interacting with the harmonic (a different kind of phase-matching). The detailed interactions are beyond the level of this chapter, but the full ramifications of third order nonlinearities were extensively discussed quite early (Armstrong, 1962; Maker, 1965; Hellwarth 1977). As soon as third harmonic is generated, the light intensity is usually high enough to generate even higher harmonics than the third and the Taylor expansion ceases to be a particularly valid way to look at these large nonlinearities. The main application of third harmonic is to reach ultraviolet (UV) wavelengths where there are few choices for lasers.

When the electric field strength of the light is high enough, optical nonlinearities can generate multiple orders with light having frequencies much greater than the original (up into the X-rays!). This is done using femtosecond pulses; proper phasing of the harmonics can lead to extremely short, extremely intense pulses, approaching attoseconds in length (10^{-18} s). This is the regime of extreme nonlinear optics (Song, 2010).

It is worth pointing out that phase-matching is not a particularly problem in gases, because their refractive indices are so small that dispersion is practically negligible. With high power short-pulse lasers, very high harmonics can be observed, out to the extreme UV (XUV, for λ < 100 nm) wavelength of 6.7 nm, which was achieved in a helium gas jet, starting with a KrF laser (Preston, 1996). The laser intensities were up to $4\text{x}10^{17}$ W/cm^2 in 380-fs pulses. This was the 37$^{\text{th}}$ harmonic.

High harmonic generation (HHG) requires high peak power, sub-picosecond lasers, which today are usually mode-locked Ti-doped sapphire (Ti:Al_2O_3) lasers. A moderate, commercially available system is capable of producing a sub-100 fs pulses with mJ pulse energies at pulse repetition frequencies of 1 kHz. This laser has revolutionized high field nonlinear optics because peak optical intensities of 10^{15} – 10^{18} W/cm^2 are routinely generated (Eden, 2004); specially designed gas jets enable maximum efficiency (Grant-Jacob, 2011). A later section will discuss special results in nonlinear media observed with pulsed lasers. Harmonic emission between 20 and 60 nm could be observed.

3.2 Nonlinear refractive index

When the nonlinear refractive index is nonlinear, the phase of the light changes. This does not require phase-matching, and so it occurs to some extent in all materials. In bulk materials, the nonlinearity in a plane wave cannot be directly observed because it is a pure phase-change. However, many geometries have proven to be important in producing nonlinear effects from the nonlinear refractive index, as will be described later. They include: 1) wave-mixing, when two plane waves intersect at angles in a nonlinear medium, which creates a phase-grating that can deflect (or reflect) light beams; 2) self-focusing or de-focusing of a beam of finite width; 3) formation of stable propagating beams called spatial solitons; 4) nonlinear waveguides; 5) nonlinear interfaces; and 6) in transient phenomena, where self-phase modulation can change monochromatic light into a frequency continuum.

The nonlinear refractive index, which depends quadratically on the light's electric field is usually written as $n(I) = n_o + n_2 I$, where I is the intensity of the light. Notice that in this nomenclature n_2 is related to χ_3. Because a nonlinear refractive index changes the phase experienced by the light, the conceptually simplest way to measure it is by interference with a reference beam. A more convenient experimental technique is wave-mixing (discussed below).

Alternatively, the nonlinear refractive index can be calculated from the Kramers-Kronig relation, which relates the nonlinear refractive index to the spectrum of nonlinear absorption, assuming the same level of excitation. The Kramers-Kronig relation states that when optical intensity I is present at frequency ν, a change in refractive index Δn can be determined by measuring the change in absorption Δα at all possible frequencies ν′, under the same excitation conditions, and integrating by means of the following equation:

$$\Delta n(\nu) = \frac{c}{2\pi^2} \mathscr{P} \int_0^\infty \frac{\Delta\alpha(\nu')}{\nu'^2 - \nu^2} d\nu'$$

where $\mathscr{P}$ denotes the principal part of the integral. Because of the resonant denominator, the nonlinear refractive index due to nonlinear absorption may be quite large near a resonance. Indeed, in some geometries, such as an etalon, the nonlinear refractive index may have a bigger effect on the light beam than nonlinear absorption. Both the nonlinear refractive index and nonlinear absorption must be considered whenever an optical nonlinearity is near an absorption line.

3.2.1 Z-scan measurements of nonlinear refractive index

If the incident laser light is a Gaussian (or other shaped) beam, the nonlinear medium will induce a lateral spatially varying refractive index that will cause the beam to change its

phase front. If the refractive index increases with intensity, an intense light beam will tend to "self-focus" as it travels through the medium (as discussed later). The nonlinear medium acts like a graded index lens. This lateral change in beam shape due to the nonlinear refractive index motivated a new technique called the *z-scan* that can measure both the magnitude and sign of the nonlinear refractive index (as well as the nonlinear absorption) (Sheik-Bahae, 1990).

In the z-scan measurement technique, a sample of the nonlinear material is moved through the focus of a laser beam, and an aperture is placed before the detector at some point in the expanding beam. The amount of light getting through this aperture is measured as a function of the sample position. If the nonlinearity is positive, the beam tends to self-focus, reducing the beam divergence and increasing the amount of light transmitted through the aperture. If the nonlinearity is negative, the amount of light will decrease. From the measured dependence of the detector signal on the sample position, it is possible to calculate the magnitude of the nonlinear index. The formula for the transmission is

$$T(\mathrm{z}) = \frac{\int_{-\infty}^{\infty} P_r(\Delta\Phi_0(t))dt}{S\int_{-\infty}^{\infty} P_i(t)dt}$$

where P_T is the transmittance power through the aperture, which is a function of the phase distortion $\Delta\Phi_o$, and P_i is the incident power. Experimental data are fit to this equation. The fitting parameters are the nonlinear refractive index, together with nonlinear absorption.

3.2.2 Mechanism of nonlinear refractive index

The third-order nonlinearity produces a term that provides a nonlinear refractive index that is quadratic in the optical field (or linear in the optical intensity). This is sometimes called the *optical Kerr effect* (OKE) because the ordinary Kerr effect describes a refractive index change that depends quadratically on *applied* electric field.

The classical picture of a nonlinear refractive index is a nonlinear polarization, driven by the electric field. The polarization is proportional to the polarizability of the medium. In the simple physical picture, this is expressed as the oscillating charge separation introduced by the oscillating electric field: a simple harmonic oscillator. When the field is intense enough – approaching the value of the internal fields within the medium – the atomic cloud distorts and the harmonic oscillator becomes nonlinear. The nonlinearities can be calculated by a virtual mixing of the states of the atom or molecule. These classical and quantum mechanical pictures offer hints as to what materials will be the most nonlinear. However, for most applications, the nonlinear refractive index is determined by measurement. It is classically written as $n = n_o + n_2 I$.

3.3 Cascading nonlinearity

It has already been pointed out that the effects at a given order of χ can be cascaded. For example, the χ_2 nonlinearity interacting with the fundamental can give rise to third harmonic. By the same token, one would expect cascading of χ_2 with the complex conjugate of the fundamental to give rise to an additional component at the fundamental frequency.

This shows up as a phase shift, which is equivalent to a nonlinear refractive index. Thus a nonlinear refractive index can be created by a cascading nonlinearity in a χ_2 material. Creating an effective χ_3 nonlinearity from χ_2 begins with phase-*mis*matched second-harmonic generation. Intensity-dependent up- and down- conversion both take place, providing an intensity-dependent phase change to the wave – thus mimicking a nonlinear refractive index. This can be understood as frequency-degenerate interactions between one wave (with itself) or two waves that induce self- or cross-phase modulation. (Stegeman, 1996; Lee, 2011)

4. Nonlinear absorption

Absorption processes can be strongly non-linear, particularly near atomic resonances. Assuming a nonlinear form of Beer's law, the intensity varies with distance z as $I = I_o\exp[a(I)z]$. The absorption coefficient α may become larger or smaller with increased intensity, depending on the physical process. Increasing absorption, even in transparent media, can come from the introduction of multi-photon absorption at high intensity levels. Reduced absorption comes from saturating the absorption line with high intensity light.

4.1 Multi-photon absorption

The absorption can be written heuristically as a function of intensity through $\alpha(I) = \alpha_o + \alpha_1 I + \alpha_2 I^2$ where α_o represents linear absorption, α_1 represents two-photon absorption, α_2 represents three-photon absorption, etc. The phenomenon of multi-photon absorption, where the absorption increases with intensity, is sometimes called *reverse saturable absorption*. Even though a material is transparent at low intensity, as the intensity grows, the absorption may increase. *Two-photon absorption*, which may occur in transparent materials, can be large when the sum of two photon energies comes close an absorption resonance (DeSalvo, 1996). This optical nonlinearity decreases the transmission of light as atoms or molecules absorb it while transitioning to higher levels. If the matrix elements allow it, these higher levels may return to the ground state by emitting fluorescence at twice the frequency of the input light. While this doesn't strictly follow the definition of nonlinear optics given in the first section, multi-photon fluorescence has become a very important tool for biological applications (Xu, 1996, Diaspro, 2006)).

Higher-order multi-photon resonant excitation processes may induce considerable absorption within the material. With enough laser intensity, it is possible to induce processes that mix quantum states of an atom or molecule at energies sufficiently high to cause ionization (Corkum, 1993; Guo, 2009). *Multi-photon ionization* is assumed to be the cause of the breakdown of air (or transparent materials) at the focal point of a high power light beam. Multi-photon absorption continues until ionization occurs and the material is damaged, often by the inclusion of microscopic bubbles. A commercial example that demonstrates this process is the transparent glass cubes (or other shapes) that can be purchased with 3D images written inside. This process is done with intersecting laser beams using multi-photon absorption that leads to ionization only where they overlap.

An important application of multi-photon absorption (or reverse saturable absorption) is *optical limiting*. This is defined as any process the limits the amount of light that can get through a material at high intensity. It has the potential application of protecting sensitive

detectors and eyes from high power lasers (Tutt, 1993; Chi 2009; Kamina, 2009). With the advent of nanocrystals, research to find practical materials has exploded, yet to date it does not appear that any particular material stands out as viable.

4.2 Saturable absorption

When the frequency of incident light is near an absorption resonance of the material, the absorption may saturate as the intensity increases. Saturable absorption occurs when the incident intensity is high enough that the ground state population is depleted and the population of the upper and lower states equalizes. Although this is a microscopic process, it is often modeled heuristically by an absorption of the form $\alpha(I) = \alpha_o I_s/(I+I_s)$, where I_s is the *saturation intensity*. Saturable absorption has a number of practical applications, particularly for Q-switching and mode-locking lasers. Because the lowest loss occurs when the laser modes are locked together into pulses, introduction of a saturable absorber into a laser cavity enables it to passively mode-lock, an important way to generate ultra-short pulses. Saturable absorbers are also useful for nonlinear filtering outside laser resonators, which can clean up pulse shapes. Saturable absorption occurs at wavelength close to a resonance. Saturable absorption is particularly strong in semiconductor lasers at wavelengths just above the band edge.

5. Nonlinear scattering processes

In addition to transmission and absorption, light transmitted through materials can exhibit scattering. The linear elastic processes are Rayleigh and Mie scattering from density fluctuations in the medium. The non-elastic processes are Raman and Brillouin scattering. Rayleigh scattering comes from molecules and fine-scale density fluctuations (this is why the sky is blue); Mie scattering from fluctuations with a larger length-scale. Because the scattering particles do not move, light-induced density fluctuations appear constant in time (if the light is a continuous wave: cw) and appear as a light-induced refractive index change. These scattering processes are usually described by the χ_3 process explained earlier, so this section concentrates only on the non-elastic processes.

5.1 Stimulated Raman Scattering (SRS)

Raman and Brillouin scattering are inelastic events; the scattered light has a different frequency from the incident light. Spontaneous Raman Scattering usually down-shifts light to lower frequencies, because molecules in the medium begin to vibrate at frequency ω_r. If there are already oscillations in the medium, the light coming out will be up-shifted by the vibrational energy ω_r. Terminology has been developed that the down-shifted scattered components are called Stokes light, while the up-shifted components are called anti-Stokes light. (Stokes had already explained that in fluorescence, emitted light should always have a lower frequency than the incident light.) Raman spectroscopy has made important contributions to chemistry because it can identify molecular vibrations and measure their frequencies. These are spontaneous scattering events that can be understood only with quantum mechanics, and they have stimulated scattering analogs.

An analogy with lasers is very useful here; spontaneous emission in lasers is quantum-mechanical, while gain can be explained classically. Similarly, Raman and Brillouin

scattering have their stimulated emission counterparts, offering gain. These processes can be understood classically when we assume that the scattered light is already present. We can then calculate the gain that the Stokes light experiences in the presence of the incident light. The existence of this gain, proportional to the incident light intensity, is what makes these nonlinear optical processes.

Assume the light field consists of incident and scattered components, E_o and E_{-1} at frequencies ω_o and ω_{-1}, respectively, where $\omega_{-1} = \omega_o - \omega_r$. When ω_r is resonant with a molecular vibration, the frequency difference between these two waves can drive a molecular vibration. As with electronic states, this excited vibration can return to its non-vibrating state by spontaneous emission, or by stimulated emission.

When the incident light is intense and coherent, the molecular vibration is strongly driven at frequency ω_r as a result of interference between the incident and Stokes light (Garmire, 1963). The molecular bond length changes by an amount $\delta x \propto (E_o^* \bullet E_{-1})$, where the fields are considered vectors. The bond length oscillates at frequency ω_r, producing an oscillating electric-dipole moment that is proportional to the incident field through $\mu \propto E\delta x \propto E\,(E_o^* \bullet E_{-1})$. The dipole moment component at frequency $\omega_o - \omega_r$ is $\mu \propto (E_o^* \bullet E_{-1})E_o$, which drives power $\mathcal{P}_{-1}$ into the first Stokes through $\mathcal{P}_{-1} = -(d\mu/dt) \bullet E^*$. This product means that the power delivered to Stokes light from the incident beam is proportional to the square of the Stokes field: $\mathcal{P}_{-1} \propto |E_{-1}E_o|^2$. In other words, the gain is proportional to $|E_o|^2$, the incident optical power.

When the gain is weak, the Stokes light is spontaneous, emitted diffusely in angle and there is no *ab initio* phase relation between the Stokes and laser beam. The coherent molecular vibrations build up with a well-defined phase only when the laser beam intensity $\propto |E_o|^2$ becomes strong. Then the gain increases rapidly with incident light. For SRS to be practical for frequency conversion, a reasonable fraction of the incident light must be down-shifted by the SRS process. If equal powers in the incident and Stokes-shifted beams are assumed, in an interaction length L, the power requirement can be expressed as $\mathcal{P}_o(L) = \mathcal{P}_{-1}(L) = 16A_{eff}g_RL$, where g_R is the Raman gain and A_{eff} is the effective area of the beam (or fiber mode).

In Raman scattering, incident light induces molecular vibrations at natural resonance frequencies ω_r. These molecules have oscillating dipole moments given by the product of the molecular polarizability α_p and the electric field. When the light is coherent, the light-matter interaction transfers the phase coherence of the light to the molecules; the oscillating dipole moments induce a polarization density in the macroscopic medium, given by $P = N\alpha_pE$, where N is the density of oscillating molecules and E is the light's electric field at the molecule. An alternative picture describes this polarization density as a nonlinear susceptibility χ through $P = \varepsilon_o\chi E$. To first order, SRS can be expressed as a quadratic nonlinear susceptibility: $\chi = \chi_1 + \chi_3E^2$, where χ_3 is assumed to be highly resonant around the Raman resonance (and imaginary) (Shen, 1965).

As for anti-Stokes, if the electric field is assumed to additionally contain the frequency $\omega_o + \omega_r$, then a coherent parametric interaction can take place. This interaction is out-of-phase relative to the incident field: $\boldsymbol{\mu} \propto (\mathbf{E_o}^* \bullet \mathbf{E_{-1}})\mathbf{E_o}^*$, which means that the anti-Stokes field drives the vibrating molecule back down to its ground state. This means that those periodic vibrations introduced into the medium by the emission of Stokes light are transferred back to the light wave in the form of coherent anti-Stokes emission – a classical resonant parametric process. For anti-Stokes to build up, the proper phase relation between the wave

vectors must be maintained: $2\mathbf{k_o} = \mathbf{k_1} + \mathbf{k_{-1}}$. When phase-matched, the power delivered to the anti-Stokes light is $\mathcal{P}_{+1} \propto (E_o^* E_{-1})(E_o^* E_{+1})$, which is linearly proportional to the anti-Stokes field. The linear proportionality means that there is no threshold – the anti-Stokes field can grow solely from the interaction between the Stokes and incident field (as long as phase-matching the relationship is obeyed). This can be thought of as a *resonant four wave mixing process*.

Stokes radiation is usually emitted more strongly in the forward direction because the interaction length between the laser and Stokes is longest for the forward-directed components. The anti-Stokes is emitted in cones that obey the required phase relation with the forward-directed Stokes. When the Raman medium is inside the laser cavity, there is no anti-Stokes because there is no Stokes emission at the appropriate angles to feed into anti-Stokes.

The simple classical picture shows that higher order Stokes can be generated either by the first Stokes generating the second Stokes in exact analogy with the generation of first Stokes, or by a four-wave mixing process in which the molecular vibration due to E_o mixes with E_{-1} to produce a dipole moment $\mu \propto (\mathbf{E_o^* \bullet E_{-1}})\mathbf{E_{-1}'^*}$, where the Stokes wave with field E_{-1}' does not have to travel in the same direction as the wave with field E_{-1}. The power generation at this second Stokes is $\mathcal{P}_{-2} \propto (E_o^* \bullet E_{-1})(E_{-1}'^* \bullet E_{-2})$**.** This process has no threshold and requires the phase-matching wave vector relationship $\mathbf{k_o - k_{-1} = k_{-1}' - k_{-2}}$. This simple model also explains higher order anti-Stokes. Radiation at frequency $\omega_{+2} = \omega_o + 2\omega_r$ is produced without threshold by modulation of the first anti-Stokes by the molecular vibration at frequency ω_r. The dipole moment $\mu \propto (\mathbf{E_o^* \bullet E_{-1}})\mathbf{E_1^*}$ drives second anti-Stokes power at $\mathcal{P}_{+2} = (E_o^* E_{-1})(E_1^* E_2)$. This requires the phase-matching wave vector relationship $\mathbf{k_o - k_{-1} = k_2 - k_1}$.

The Raman gain is usually measured experimentally, and will be proportional to the spontaneous emission spectrum (as is true with lasers). Raman lasers occur when the laser-pumped Raman-active gain medium is placed between mirrors that reflect the first Stokes wavelength. Again, this is analogous to lasers, where the gain medium must be placed inside a cavity to achieve laser threshold. On the other hand, the Raman gain is very large, and can build up from noise to a substantial signal without any feedback. This strength makes SRS in Raman-active liquids very strong, and explains the deleterious SRS that builds up in fibers. Once the first Stokes has built up to a substantial signal, all the other wavelengths can build up from it by parametric processes.

Using solid-state terminology, molecular vibrations are optical phonons. With this point of view, it is reasonable to expect optically-excited acoustic phonons to have their stimulated counterpart. This is Stimulated Brillouin scattering, which will be discussed in the next section, but first we'll look at some SRS applications.

5.2 Applications of Stimulated Raman Scattering

A few exciting possibilities made possible with SRS are mentioned here. In most cases the value of SRS is that is produces coherent light at frequencies other than those available directly from known lasers. In fibers, where intense light travels for a long distance down a Raman-active medium (fused silica), SRS can build up and be detrimental by shifting the wavelength of the incident light. This is a problem in optical fibers for telecommunications and for flexible delivery of high-intensity light, although it is an advantage when the Raman light can be used as an amplifier. Spectroscopy is another field in which SRS has been particularly useful.

5.2.1 Raman lasers

Raman lasers come in many designs for obtaining new frequencies that are not produced by lasers themselves. The way to achieve Raman threshold with the lowest optical intensity is to put the Raman medium inside the laser cavity, utilizing the same cavity mirrors as the laser (with reflectivity at both the laser and Raman frequencies). For example, yellow light at 590 nm is a difficult laser color to produce, but can be achieved by frequency-doubling coherent light at 1180 nm with a KTP crystal. What source gives light at 1180 nm wavelength? A Raman laser from a barium tungstate ($BaWO_4$) Raman crystal placed inside a linear-cavity repetitively *Q*-switched diode-side-pumped Nd:YAG laser at 1064 nm. An average output of 3.14 W at 590 nm has been achieved (Li, 2007).

Hydrogen and methane under pressure offer the largest Raman shifts of all molecules and are used to obtain high-power pulsed lasers at new frequencies. For example, a frequency-doubled YAG laser Raman-shifted with methane provides output at 630 nm. Pressurized gases can be used in single pass, Raman resonator, oscillator-amplifier, and/or waveguide design; they don't have the self-focusing, Brillouin and anti-Stokes that solids have. They may be intra-cavity or extra-cavity.

Parametric Raman lasers can achieve efficient generation of both the second order Stokes and first anti-Stokes components emitting nearly diffraction-limited collimated beams. A first Raman laser is excited by some of the laser pump energy and produces a 1st Stokes component as a collimated beam. In the parametric Raman laser the Stokes beam interacts parametrically with the remaining collimated pump beam to produce high power (Grasiuk, 2004).

Raman lasers in silicon offer light generation within integrated circuit technology for intra-chip and chip-to-chip information transmittal. Raman lasers in silicon use a CW pump beam from a laser diode and have the first-Stokes laser mirrors integrated right into the silicon chip (Service, 2005), a technique necessitated because silicon itself cannot be made into a laser. Long-wavelength injection Raman lasers are composed of alloys of aluminum, gallium, indium, and arsenic. These Raman lasers are grown on a single chip; some layers convert electricity into an initial pump laser and other layers shift the light via first Stokes to longer wavelength, out to 9 μm (Troccoli, 2005).

5.2.2 SRS in fibers

The existence of SRS can be a problem in fiber optics, where over long distances it may broaden transmitted spectra. In other cases, SRS gain can be very useful, as an amplifier of weak signals, such as used in telecommunication systems. A Raman laser results when an SRS medium is placed in an optical cavity.

Stimulated Raman scattering places a serious limit to delivering power down a fiber. As shown earlier, the effective SRS threshold is $\mathcal{P}_{-1th} = 16\, A_{eff}\, g_R\, L_{eff}$, where now A_{eff} is the effective mode area of the fiber and L_{eff} is the length over which the SRS takes place. Larger mode area fibers enable more power to be sent down a given length without SRS becoming a problem, but they are not usually single mode, and aren't used in telecommunications. The Raman gain coefficient $g_R \sim 10^{-13}$ W/m for silica fibers (and polarized light).

While often detrimental, the SRS gain in fibers can be useful by providing a Raman amplifier, sometimes used in telecommunications. Distributed amplification is particularly

appealing because it requires only a single pump source for all of the structure, reducing the network's cost and complexity. The down-side is that Raman amplification tends to require significant input powers. Distributed Raman amplification is applied in long-haul, broadband transmission systems that use wavelength division multiplexing (WDM) because amplifiers must provide a flat gain profile for all the signal channels. Raman amplifiers enable control over the Raman gain profile, and thereby reduce amplified spontaneous scattering noise. Adding a fiber Raman amplifier to a fiber Erbium amplifier offers a much wider gain bandwidth than either component alone (Islam, 2004; Headley, 2005).

Raman fiber lasers, with feedback to turn the amplifier into a laser, have potential applications in WDM systems, optical fiber sensors and spectroscopy. Continuously tunable channel spacing can be achieved with a hybrid of an erbium-doped fiber laser that gives high power conversion efficiency and a fiber Raman laser that has a large lasing bandwidth, both placed in an all-fiber ring cavity (Chen, 2007); stable multi-wavelength lasing has been observed over 24 wavelengths.

5.2.3 Stimulated Raman Spectroscopy

The nonlinear process of SRS provides a way to enhance the Raman signal for spectroscopic applications. The most common method is often called *CARS (Coherent anti-Stokes Raman Spectroscopy)*. Light at both the laser and first Stokes frequencies are incident on the Raman-active medium and the beating between these two laser beams sets up coherent molecular vibrations that parametrically generate the anti-Stokes frequency (Begley, 1974). This resonant four-wave mixing phenomenon obeys the usual requirement for phase-matching. The conversion efficiency from Stokes into anti-Stokes is proportional to the laser intensity squared, enabling as much as 10^5 times increase in the conversion efficiency. This method is particularly useful for investigating biological compounds where background fluorescence is a problem for conventional spontaneous Raman studies. CARS does, however, require a high power tunable laser (or an optical parametric amplifier). The spectroscopic techniques that use SRS are described in books and papers (Demtroder, 2008, McCamant, 2004).

Other stimulated Raman spectroscopy topics under study include transient behavior, Raman lasers, waveguides and fibers, and SRS at surfaces and in cavities. The ability of SRS to provide frequencies as needed has enabled coherent atom control (Hagley, 1999; Lukin, 2003) and manipulating quantum states (Bergmann, 1998; Scala, 2011).

5.3 Stimulated Brillouin Scattering (SBS)

In solid state physics, Raman-induced vibrations can be described as optical phonons. Interaction of light with acoustic phonons results in Brillouin scattering (the acoustic phonons are actually hypersonic, i.e. very high frequency acoustic waves). SBS can be understood, then, as a straight-forward extension of SRS to acoustic rather than optical phonons. SBS gain occurs in similarity with SRS. Stimulated Brillouin scattering occurs when two optical waves interact in materials through an acoustic wave generated by electrostriction. Electrostriction is the tendency of materials to become compressed in the presence of an electric field; electric fields change the density and therefore refractive index of electrostrictive materials. Spontaneous Brillouin scattering was known previously, just as spontaneous Raman scattering had been known before lasers. As with SRS, the spontaneous

process is best explained quantum mechanically; an incident photon of energy $h\nu_o$ is scattered by an acoustic phonon of energy $h\nu_a$, and energy conservation requires that the scattered photon has an energy given by $h\nu_{-1} = h\nu - h_a\nu$. On the other hand *stimulated* Brillouin scattering can be explained classically as the beating of the electric fields of two optical waves that generate a hypersonic wave through electrostriction. This causes a moving index grating that scatters an incident optical wave and is the origin of the nonlinear coupling between the waves. The scattered wave frequency will down-shift or up-shift, depending on whether the acoustic phonon takes energy from the incident photon $h(\nu_o - \nu_a)$ or gives its energy up to the incident photon $h(\nu_o + \nu_a)$, respectively. There is a strong thermal excitation of acoustic phonons because the Brillouin shift is very small, so anti-Stokes up-shifted scattered light is comparable in intensity to Stokes down-shifted light. Typical Brillouin shifts are in the GHz regime. For example, the shift in optical fiber at wavelengths near 1.55 μm is ~ 9.6 GHz.

While SRS frequency shifts are given by fundamental characteristics of the scattering molecules and first Stokes has no phase-matching requirement, in SBS the acoustic frequency that determines the Stokes frequency shift is determined by a phase-matching requirement. This is because Raman-excited vibrations are localized on molecules, while Brillouin excitations are pressure waves that move with acoustic velocity v_a. The requirement that the hypersonic waves remain in phase with the interfering light waves provides the following vector relation: $\mathbf{k}_{-1} = \mathbf{k}_o - \mathbf{k}_a$. For the incident and scattered light to be in the same direction, the acoustic frequency would have to be zero. Because the magnitude of each vector is inversely proportional its velocity and the acoustic wave is much slower than the light waves (by a factor of 10^{-5}), the acoustic wave vector will be much larger than the optical wave vector, unless that acoustic frequency shift is very small. The largest the frequency shift occurs when the Stokes wave travels opposite the incident wave. In this case $\omega_a/\omega_o = 2nv_a/c$, which is in the multi-GHz range.

5.3.1 SBS retro-reflection

The retro-reflection that occurs with SBS is perhaps its most important characteristic. The first experimental results on SBS excited in liquids (with a ruby laser) showed that the retro-reflected Stokes light returned to the (inhomogeneously broadened) laser, where this new frequency was amplified and reflected back to the liquid. Another SBS step then produced twice-shifted light (Garmire, 1964). It was only later that it was understood that *phase-conjugation* was taking place. A normal mirror changes the phase of the incident light upon reflection by π. Brillouin-reflected light, on the other hand, has a phase that is conjugate to that would be reflected off a usual mirror. This explains why SBS light could retrace its steps back into the laser, even after traveling through a lens.

To understand phase conjugation, consider the susceptibility that oscillates with the acoustic frequency by beating with a forward incident wave field $E_o = \mathcal{E}_o \exp[i(\omega t - kz)]$ and a backward-directed Brillouin wave field $E_{-1} = \mathcal{E}_{-1} \exp\{i[(\omega-\omega_r)t + k_{-1}z)]\}$. Considering complex notation, the term which gives the appropriate oscillation frequency for the susceptibility is $\chi = E_o E_{-1}^*$, which oscillates at frequency ω_r, and has a rapid periodicity in z, due to the propagation of vector $\mathbf{k}+\mathbf{k}_{-1}$. The result is

$$\chi = \mathcal{E}_o\mathcal{E}_{-1}^* \exp\{i[\omega_r t - (k_{-1} + k)z]\}.$$

The oscillating polarization that drives the backward wave E_{-1} is given by

$$P = \varepsilon_o \chi E_o^* = \varepsilon_o \mathcal{E}_o \mathcal{E}_o^* \mathcal{E}_{-1}^* \exp\{-i[(\omega - \omega_r)t + k_{-1} z]\}.$$

This a backward going traveling wave with a phase π different from the initial backward-going wave. This means the phase of this polarization density is conjugate from the initial Stokes field. This is the origin of the term "phase conjugation."

The "magic" of phase conjugation can be explained by looking at what the phase does for any wave leaving a point (x,y,z) on one side of the Brillouin phase conjugator. Assume the wave builds up a phase φ as it travels to the conjugator; when it reflects back, its phase in conjugated. That is, the phase φ becomes –φ. As that wave retro-reflects back to the point (x,y,z), it re-traces its steps and its phase returns to zero. This happens for every point, no matter what the phase distribution is between its and the conjugator. Thus any aberrations are completely cancelled out. If this were an ordinary mirror, the phase would *increase* from φ to 2φ upon a round-trip, rather than returning to zero. Thus the aberration *adds* for an ordinary mirror and *cancels* for a phase-conjugate mirror.

Nonlinear phase conjugation was first understood in the context of SBS and quickly was extended to other materials and processes, particularly photo-refractives, while SBS has remained a valuable way to reduce aberrations in high pulsed power applications, described later.

5.3.2 Performance limitations due to stimulated Brillouin scattering

In fiber telecommunications SBS puts a limit on the power that can be transmitted through fibers that is even more stringent than SRS. If the light in the fiber is too intense, SBS reflects light back where it came from, shifted down in frequency by the Brillouin acoustic vibration. This reduces the power that can be transmitted through single mode fibers for telecom applications (Shiraki, 1996). There is not a lot of flexibility in the design of telecommunications fibers because of requirements for low loss and low dispersion. The SBS gain G_B and threshold input (monochromatic) power $\mathcal{P}_{th}$ through a fiber of effective area A_{eff}, respectively, are given by:

$$G_B = (4\pi n_{eff}^8 p_{12}^2/\lambda^3 \rho c v \Delta v_a)(\mathcal{P}_o/A_{eff}) \text{ and } \mathcal{P}_{th} = 21\, A_{eff}/g_B L_{eff}$$

where n_{deff} is the effective refractive index, p_{12} is the longitudinal elasto-optic coefficient, ρ is the density, c is the velocity of light (λ and v are the wavelength and frequency of the incident light, respectively), L_{eff} is the effective interaction length and Δv is the linewidth of the acoustic resonance (Kobyakov, 2005). The usual approach to reducing the effect of SBS is to use frequency-broadened pulses that smear the SBS gain over a range of wavelengths.

The gain is proportional to the intensity, $(\mathcal{P}_o/A_{eff})$, as expected and proportional to the square of the elasto-optic coefficient. In narrow line fiber lasers and amplifiers, SBS remains the primary limitation on output power. Large mode area fibers decrease the optical intensity in the fiber core and raise the SBS threshold, but the maximum output power from narrow linewidth optical fiber amplifiers is still limited to approximately 100 Watts. Because SBS in an optical fiber occurs when the signal propagating in the core generates an acoustic wave that scatters light in the reverse direction, the SBS threshold can be raised by choosing a refractive index profile that minimizes the acousto-optic overlap while maintaining the

desired optical properties (Kobyakov, 2005). Doping the core of the fiber with alumina (Al_2O_3) creates an optical waveguide but an acoustic anti-guide. Combining alumina and germania (GeO_2) doping in the fiber core can spatially separate the optical and acoustic fields, yielding over 500 Watts of power in a single-mode output, without the onset of SBS.

In laser-produced plasmas, SBS can be set up by thermal waves. In low-temperature, high-density high-Z plasmas this instability dominates and can produce significantly more SBS that expected (Short, 1992).

5.4 Applications of Stimulated Brillouin Scattering

Possible applications of SBS are too numerous to describe in detail. Indeed, several books on SBS have already been written (Damzen, 2003; Agrawal, 2008), describing the problems it causes in practical systems and how to overcome them, but also how SBS can be used to improve other systems. These positive applications broadly can be thought of as improving lasers and as improving sensing systems.

A phase conjugate mirror corrects wavefront aberrations, compensating for distortions of the laser beam created by inhomogeneities in the laser medium and/or its optical components. The SBS phase conjugate mirror is the simplest means to create phase-conjugation and is suitable for high power/energy laser systems. One problem needing correction by this means is thermal lensing caused by inefficient optical pumping of Nd:YAG lasers (Kovalev, 2005).

Phase conjugate mirrors are excellent for beam combining, although SBS requires the multiple lasers to be within the Brillouin gain linewidth. SBS phase conjugation is appropriate for combining beams from an amplifier array (Bowers, 1997). Research continues on how to combine the many beams needed for laser fusion (Kirkwood, 2011).

SBS can help clean up laser beams, because the backward-going Stokes has a much smoother beam profile than the incident laser beam. Thus it is sometimes practical, for example if using a multi-mode fiber, to use the output from a retro-reflected Stokes beam rather than the original laser beam **(**Steinhausser, 2007).

The SBS effect in a fiber ring sets up an acoustic wave that remains stable as the laser light beam travels around the ring, as long as the wavelength of the laser and the circumference of the ring are carefully matched. This enables the Brillouin laser to have an extremely narrow line, as narrow as 75 Hz (Geng, 2006).

Brillouin scattering depends on strain and temperature, making possible distributed sensing through Brillouin scattering in optical fibers. Brillouin enhanced sensing optical fibers can be imbedded in smart composites. The backward scattered Brillouin wave can travel over long fibers as an indicator of where the fiber is undergoing strain or other problems. One technique involves introducing pump and probe at both ends and doing an optical correlation. Both stimulated and spontaneous Brillouin scattering have been used for these applications (Horiguchi, 1995; Bao. 2011).

Laser pulse compression by SBS involves a tapered waveguide within a cell of pressurized methane gas. The Stokes pulses in the backward direction are compressed from incident nanosecond laser pulses (Hon, 1980). The taper ensures SBS starts at the far end of the cell

and the transient dynamics between the incident, reflected and pressure wave all combine to reduce pulses to sub-nanosecond. With two cells in a generator-amplifier setup, up to 25 J in 15 ns pulses have been compressed to 600 ps (Dane, 1994); the two-stage process is much more stable than one alone (Erokhin, 2010).

SBS in photonic crystal fibers (PCF) can be dramatically altered by wavelength-scale periodic microstructuring, which alters both the optical and the acoustic properties. A PCF guides light through a lattice of hollow micro/nano channels running axially along its length. These fibers can be designed to either eliminate SBS or to increase it. The acoustic changes are particularly significant in fibers that contain filamentary voids. In one such example, the SBS threshold was increased five times when the Stokes frequency shift was in the 10-GHz range (Dainese, 2006).

6. Nonlocal optical/Photorefractive nonlinearities

Nonlocal phenomena occur when intense light entering the medium at one location in space changes the refractive index or absorption at nearby locations. Most typically this is due to diffusion of optically-induced excitation away from the initial point of excitation. A simple example is thermal nonlinearities, observed when thermal heating due to absorption of laser power spreads to adjacent areas, effecting the whole beam, not must the most intense parts of the beam. This was observed in increasing absorption in ZnSe waveguides, which exhibited optical bistability, which could not have occurred without the non-local nonlinearity (Kim, 1987). Most often, thermal nonlinearities cause *blooming* – in which a powerful beam spreads out ("blooms") because heating lowers the refractive index where the absorption of light is the strongest (in the center of the beam) – acting as a negative lens (Smith, 1977). The other main origin of non-local nonlinearities is the transport of optically induced charges in electro-optic media, which alter the refractive index. When this effect is detrimental, it is usually called "optical damage;" it ruins the spatial profile of the Gaussian beam. When these nonlinearities are wanted, to explore new phenomena, it is called *photorefractivity*.

6.1 Optical damage

High-power lasers can cause catastrophic optical damage by means of local bubble or crack formation, usually as a result of multi-photon ionization. The term *optical* damage is also used for non-catastrophic effects that medium-power lasers can introduce in electro-optic media. Such "damage" causes refractive index gradients that cause the beam to deform, interfering with its spatial profile or its waveguide properties (Mueller, 1984). This has been a particular problem in second harmonic generation, where the non-centrosymmetry requirement is also true for electro-optic coefficients. When it is useful, "optical damage" is typically called *photorefraction*; defects or atomic impurities in these crystals causes weak absorption of the light, liberating electrons which are free to move in the crystal, either by diffusion or drift. This separation of charges that occurs with the movement of electrons, creates internal electrical fields that, in turn, alter the refractive index of these electro-optic crystals. The altered refractive index affects the propagation of the light through the crystal.

The ability of light beams to create electric fields through charge separation is called the *photovoltaic effect*. The photovoltaic effect is most deleterious when the material is strongly insulating. Providing weak paths of conduction can remove the charge separation and the

resulting photorefractivity. In $LiNbO_3$, addition of small amounts of MgO has been shown to reduce photo-refractivity by increasing conductivity.

6.2 Photorefractivity

In photorefractivity, the refractive index is locally modified by nearby spatial variations of the light intensity. Unusual new effects can be observed as a result of photo-excited carriers moving about in electro-optic crystals, due either to diffusion or to drift in local electric fields. The strongest effects are observed when coherent waves interfere to form a spatially varying pattern of illumination. As a result of photo-excited charge migration, a space charge is introduced that results in an electric field that changes the refractive index via the electro-optic effect (Cronin-Golomb, 1984). Two light beams interfering in a photorefractive medium generate photo-carriers in the spatially periodic bright regions. These carriers move to the spatially periodic dark regions where they are trapped. These trapped charges introduce a periodic electric field that creates a periodic refractive index distribution if the material is electro-optic. This refractive index grating is spatially shifted from the incident interference pattern and can diffract light into new directions. This can occur at quite low optical power levels, although it may take some time for substantial charge distributions to build up. Applications include two-beam coupling, dynamic holography, phase conjugation and spatial solution formation (Gunter, 1982).

Photo-refractivity was first discovered in lithium niobate, where it was shown that holograms could be written in real-time in the crystal, which offered promise for image processing. New crystals were investigated for photorefractivity and barium titanate was found to be have a large nonlinearity, resulting in interesting nonlinear effects, particularly related to phase conjugation. Photorefractive crystals have the advantage of high sensitivity, but tend to be very slow. In barium titanate the effects take seconds to build up; also it is sensitive only in the blue (Chang, 1985; Feinberg, 1980).

Photorefractivity has been extended to semi-insulating III-V and II-VI semiconductors, where the effect is not as large, but can be a thousand times faster, and the light source can be in the infrared – even at a wavelength of 1.55 microns in CdTe (Partovi, 1990). The largest effects require kilovolts to be applied to the crystal, but kilohertz response can be achieved. If the wavelength is near the band edge of the semiconductor, the local resonant nonlinear refractive index can add to the non-local electro-optic refractive index change to enhance the photorefractivity (Partovi, 1991). Wave-mixing can be observed with mW of incident power (Nolte, 1999).

More recently photorefractive polymers have proved effective, with the potential of low cost real-time holography (Ostroverkhova, 2004).

6.3 Photo-refractive materials

In the photorefractive effect, the local index of refraction is modified by spatial variations of the light intensity. It is typically most useful when coherent beams interfere with each other to form a spatially varying pattern of illumination. As a result, charge carriers are produced in the material, which migrate owing to drift or diffusion and space charge separation effects. The resulting electric field that is produced induces a refractive index change via the electro-optic effect. Materials must have a large electro-optic and photo-induced charge carriers.

6.3.1 Photorefractive crystals

The least expensive and commonly used photorefractive crystal, which has been around for a long time, is iron-doped lithium niobate ($Fe:LiNbO_3$), which can also be doped with titanium or cerium. It has large electro-optical (EO) coefficients, high photorefractive sensitivity and diffraction efficiency, but the photorefractive effect in this material is very slow, because charge transport is slow. Photo-refractive phase-conjugation was first observed in Barium Titanate ($BaTiO_3$). Because it is difficult to grow and delicate to handle, barium titanate has largely been supplanted by other, more practical, crystals. Lithium niobate, for example, is more suitable for volume fabrication and practical devices.

Strontium-Barium Niobate ($Sr_xBa_{(1-x)}Nb_2O_6$) SBN is an excellent optical and photorefractive material which can be nominally pure or doped with Ce, Cr, Co or Fe. SBN has a large electro-optic coefficient delivering a fast response time and high two- wavelength mixing gain. Its figure of merit for photorefractive applications is much larger than lithium niobate, opening the way to much smaller devices. No applied field is required to enhance two-beam coupling.

Sillenite single-crystal bismuth silicon oxide $Bi_{12}SiO_{20}$ (BSO) and bismuth germanium oxide $Bi_{12}GeO_{20}$ (BGO) show a unique combination of different physical properties. These are the fastest photorefractive crystals to date. The coupling gain can be enhanced by applying an external electric field. The cubic crystalline structure is enables polarization manipulation in 2 and 4 wave mixing configurations. The crystals are very efficient photoconductors with low dark conductivity that allows a build-up of large photo-induced space-charges. These materials make possible a wide range of optical devices and systems for spatial light modulators, dynamic real-time hologram recording devices, phase conjugation wave-mixing, optical correlators, and optical laser systems for adaptive correction of ultrashort light pulses. These materials can be produced as thin-film structures for optical waveguide and integrated optical devices, as well as in bulk.

6.3.2 Photorefractive semiconductors

Several semi-insulating compound semiconductors have been demonstrated to be photorefractive. They include undopcd and chromium-doped gallium arsenide (GaAs, GaAs:Cr), iron-doped and titanium-doped indium phosphide (Fe:InP, Ti:InP), undoped gallium phosphide (GaP) and vanadium- and titanium-doped cadmium telluride (CdTe:V, CdTe:Ti). These photorefractive semiconductors provide several attractive features for information-processing applications and could lead to a new generation of integrated optical information processors.

The semiconductor material must have adequate densities of localized energy levels to act as donors and acceptors for supplying and receiving the transferred charges, respectively. Furthermore, the photorefractive material has to be insulating or semi-insulating in order to avoid Coulomb screening around the charged centers. Typical resistivity of semi-insulating GaAs is higher than InP, due to its higher bandgap; semi-insulating CdTe has even higher resistivity. A commonly used figure of merit is n^3r/ε, where r is the electro-optic coefficient. The figures of merit for GaAs, GaP, lnP, and CdTe are 3.3, 3.7, 4.1, and 16, respectively. Other crystals, BSO, SBN, $BaTiO_3$, $LiNbO_3$ and $KNbO_3$, have figures of merit of 1.8, 4.8, 4.9, 11, and 14, respectively. CdTe has the highest figure of merit among all the materials listed

here. In many of the semiconductors, photo-refractivity can be larger if an external field is applied. The big advantage of semiconductors is that their response time is high; they turn off much more rapidly than the crystals. (The turn-on time depends on incident intensity.)

6.3.3 Photorefractive organic materials

The main classes of photorefractive (PR) organic materials include polymer composites, small molecular weight glasses, fully-functionalized polymers, polymer-dispersed liquid crystals, liquid crystals and hybrid organic-inorganic composites. The best performing photorefractive organic materials exhibit two-beam coupling gain coefficients Γ = 200-400 cm^{-1}, giving nearly 100% diffraction efficiencies in rather thin films. Their grating formation times are on the order of several milliseconds (Eralp, 2006). The advantage of polymer composites is the ability to tune their photorefractive properties by varying the concentration and type of constituents. However, because many components are combined in the composites, phase separation and crystallization can reduce the shelf life of devices. Also, while adding a plasticizer enhances chromophore orientation, it also increases the inert volume, which reduces overall photorefractivity (Grazulevicius, 2003; Marder, 1997). Organic glasses resolve these issues, but reduce the flexibility to tune the material's properties (Zhang, 2011). Both the shelf life of photorefractive polymers and the quality of starting materials available remain problems that have until now kept photorefractive organic materials as research materials.

6.4 Photo-refractive applications

Proposed applications include read-time holography, optical image processing, high density optical data storage, optical computing, communications, image processing, neural networks, associative memories, phase conjugation, laser resonators, and many others. Image processing applications include image correlation, image amplification, and dynamic novelty filtering. Data can be stored in photorefractive materials in the form of 3D phase holograms that have very high density and fast parallel optical access. Phase-conjugation has been used to correct image distortions suffered by optical beams in inhomogeneous or turbulent media. Photorefractive crystals, semi-insulating semiconductors, and polymer films have all been used to demonstrate proposed applications, but there remain no widespread commercial applications, due to the high cost of quality crystals and performance limitations, particularly the slow hologram formation speed in most materials.

Some photorefractive applications are on the horizon. Perhaps one of the most exciting is real-time holography that can display people, objects or scenes in three dimensions. The holograms can be seen with the unassisted eye and are similar to how humans see their actual environment. The concept of 3D telepresence, a real-time dynamic hologram depicting a scene occurring somewhere else, is surey an application with promise. A holographic stereographic technique is used, along with a photorefractive polymer material as the recording medium. The holographic display refreshes images every two seconds. A 50 Hz nanosecond pulsed laser writes holographic pixels. Multicoloured holographic 3D images are produced by using angular multiplexing, and the full parallax display employs spatial multiplexing (Blanche, 2010). Such applications will certainly increase in the future as materials become better.

6.5 Charge transport nonlinearities

A range of other nonlinear phenomena depend on the spatial transport of optically induced charge carriers within internal electric fields, particularly in semiconductor devices (Garmire, 1989). Schottky barriers and *pn* junctions provide internal fields that can be depleted by motion of photo-carriers, offering exquisitely sensitive nonlinearities through the electro-optic effect and through band-filling (Dohler, 1986; Jokerst, 1988). The modulation-doped n-i-p-i and hetero-n-i-p-i structures are examples, with the nonlinear refractive index due to resonant phenomena that can respond in milliseconds to microwatts of optical power (Kost, 1988).

7. Wave-mixing in nonlinear materials

Wave-mixing geometries involve two or more plane-waves, incident at an angle in a bulk nonlinear medium. The nonlinearity can be absorptive or it can rely on a nonlinear refractive index (or both). When the medium is photo-refractive, with mobile optically-excited charge carriers, the phenomena are particularly interesting.

7.1 Two-beam coupling

When two coherent beams interfere in a nonlinear medium, their interference introduces a grating in absorption or refractive index inside the material. These beams do not interact if the optical nonlinearity is local; they merely pass through each other. If photo-induced charges move within the material, however, a grating is set up that moves laterally with respect to the incident beams. This grating can diffract one beam into the other. The direction of energy transfer is determined by the sign of the mobile charge carriers and the electro-optic response. The energy transfer direction can be reversed by changing the polarity of the electric field (Partovi, 1987; Kim, 2011).

Two-beam coupling makes possible the amplification of a weak beam by means of coupling from a strong beam. Analysis of the coupled mode equations shows that the ratio of the weak beam to the strong beam increases exponentially with two-beam-coupling gain-length product ΓL:

$$I_{wo}/I_{so} = (I_{wi}/I_{si})\exp(-\Gamma L) \text{ where } \Gamma = (4\pi/\lambda)(\Delta n/m)\sin\Phi.$$

where I_{wo} and I_{so} are the weak and strong output beams, respectively, and I_{wi} and I_{si} are the weak and strong incident beams, respectively. Δn is the peak nonlinear refractive index introduced by the interference, m is the diffraction order, and Φ is the lateral phase angle between the periodic spatial intensity profile and the refractive index grating (that was moved by photo-charge transport). The gain can be used as a polarization-converter if the unwanted polarization is used to drive the gain (Heebner, 2000).

Beam coupling has been observed in the conventional photo-refractive crystals such as barium titanate and Fe:$LiNbO_3$. Some possible applications are optical limiting, produced by some fraction of the pump beam being reflected back onto itself, thereby robbing the incident beam if it becomes too powerful.

7.2 Three-wave mixing

Parametric processes involve three waves interacting. An example is parametric down-conversion, which is at the heart of the optical parametric oscillator (OPO) that will be

discussed later. In a χ_2 medium, each incident pump photon breaks up into two less-energetic photons (the signal and the idler) such that the sum of their energies equals that of the pump photon. The sum of the signal and idler wave-vectors must also equal that of the pump ("phase-matching," as required in second-harmonic generation).

Parametric down-conversion can be regarded as the inverse process of sum-frequency generation, in which two beams at different frequencies create a beam that has a frequency equal to the sum of their frequencies. Thus sum- and difference- frequency processes are also three-wave mixing processes. In difference-frequency generation, it can be considered that both the pump beam and an intense idler beam mix create the signal beam. In parametric generation, the idler signal builds up from noise and feeds the signal beam with a gain per unit length. This process is enhanced by providing a cavity for the signal beam, in which case it has a threshold and becomes an optical parametric oscillator (OPO). These processes are particularly important to reach wavelengths in the mid-infrared.

The mixing of an anti-Stokes Raman wave with the laser beam and a Stokes wave is another three-wave mixing process. These processes do not have thresholds (unless they are placed in cavities). Three-wave mixing can even be used for generating holograms (Bondani, 2002). Three-wave mixing can be effectively applied to wavelength conversion, all-optical gating, all-optical switching, optical parametric amplification and oscillation, where it can increase the wavelength range over which these applications can operate (Liu, 2002).

7.3 Four-wave mixing

Four-wave mixing is a nonlinear effect arising from a third-order optical nonlinearity, χ_3. The four-wave mixing (FWM) geometry is similar to two-beam coupling: two incident (or "pump") beams (or "waves") "write" an optically-induced grating by means of nonlinear refractive index, non-linear absorption, or both. In FWM there is also a probe, or reading, wave that is partially diffracted from the optically induced grating to form a fourth wave, called the "signal beam." In the degenerate FWM geometry (DFWM), all four beams have the same wavelength. FWM provides background-free detection of very weak diffraction signals, since the signal wave appears at a different angle from the rest of the light.

The diffracted beam intensity (signal) is typically measured as a function of time, applied electric field, writing beam intensities, etc and the diffraction efficiency is determined. Typically the probing beam should not disturb the grating, which is achieved by making the probe beam much weaker than the pump beams and/or by having the probe beam polarized orthogonal to the writing beams. In the approximation of thick (volume) grating, the diffraction efficiency (signal intensity divided by incident intensity) in a sample of length L is given by:

$$\eta = \exp(-\alpha L)\sin^2(\pi \Delta n L/\lambda)$$

where αL is any residual (linear) absorption and Δn is the maximum amplitude of the refractive index grating, where it is assumed that the incident and diffracted fields are parallel. Note that when the refractive index modulation Δn is small, the diffraction efficiency is proportional to $(\Delta nL)^2$.

If the two waves that interfere are at the same frequency, the grating is stationary. In the thick grating limit, the Bragg condition must be satisfied, so in DFWM the probe beam must

enter at the same angle as one of the pump beams. If DFWM takes place in a thin film, then the Raman-Nath condition holds and the probe beam can be at any angle. If the probe beam is a different frequency from the pumps and the grating is thick, the Bragg angle must be chosen: $\sin\theta_{probe} = n\lambda_{probe}/2d$, where d is the grating spacing caused by interference of the two pump beams.

When the two pump beams are at different frequencies, then the refractive index grating will move back and forth laterally. The probe-wave reflecting off this grating will be frequency-shifted by the frequency of the moving grating, just as in an acousto-optic modulator.

Many FWM experiments are possible: FWM measures lifetimes of gratings, spatial motions, surface effects, etc. (Abeeluck, 2002). Pulsed pump and probe waves, with a time delay between them, is a particularly valuable way to measure transient phenomena, both excited state lifetimes and dephasing (Yang, 1994). Many optical nonlinearities can be explained under the general concept of FWM, such as some third harmonic processes, SRS, SBS, parametric amplification, photo-refractive effect, and self-phase modulation (discussed later). The concept is useful to understanding a variety of spectroscopic tools, also discussed later. The most significant of these is CARS (coherent anti-Stokes Raman spectroscopy) where two input waves generate a detected signal with slightly higher optical frequency due to internal molecular vibrations. With a variable time delay between the input beams, it is also possible to measure excited-state lifetimes and dephasing rates (Becerra, 2010).

In fibers, FWM can be both a blessing and a curse. Non-degenerate FWM occurs in a fiber when two or more different frequencies propagate together, due to the fact that doped silica has a χ_3. With two input frequencies, a refractive index modulation at the difference frequency occurs, which creates two additional frequency components as sidebands on the initial waves. If there is already light at these sideband frequencies, it can be amplified, i.e., it experiences parametric amplification. In this way FWM may be a detriment to optical communications. As with SRS and SBS, FWM can be useful or harmful, depending on the application. Four-wave mixing in fibers is related to self-phase modulation and cross-phase modulation, transient effects that will be discussed later; this leads to spectral broadening that is particularly deleterious to WDM (wavelength division multiplexing), where it can cause cross-talk between different wavelength channels, and/or an imbalance of channel powers. One way to suppress this is to avoid equidistant channel spacing.

7.4 Phase conjugation and its applications

When two waves are counterpropagating ($\mathbf{k}_1 = -\mathbf{k}_2$) in a nonlinear medium, their interference sets up a grating with a periodicity of a half-wavelength. When a third wave at the same frequency is incident on this grating, the fourth wave that constitutes its reflection ($\mathbf{k}_4 = -\mathbf{k}_3$) will be the phase conjugate of the third wave. As discussed in SBS, where phase-conjugation is also seen, phase conjugation results in a retroreflection that overcomes aberrations. Photorefractive materials enable phase conjugation at relatively low optical power levels (Yariv, 1978).

The phase-conjugating grating exactly reverses the phase of any third wave. Thus, if a beam has gone through an aberration and forms a distorted wave, each portion of this wave will have its phase reversed upon reflection, so that its path will exactly reverse, re-creating the

original beam's spatial profile after the waves pass through the aberrator. This phenomenon occurs in SBS and also in photorefractive materials.

Practical applications considered for phase conjugation include correcting wavefront aberrations in a laser beam (Bach, 2010). In optical beam clean-up, the signal beam that contains information about the object is combined with the reference beam in a photorefractive material, and a volume hologram of the object is recorded. If the signal beam went through an aberrator (which would correspond to the situation when the object has to be imaged through a medium with turbulence, refractive index inhomogeneities, etc.), then the image would be heavily distorted. If, however, a reading beam counterpropagating to the reference beam is introduced, it generates the phase-conjugated replica of the signal beam, which retraces its path through the aberrator, creating a cleaned-up image of the object. Impressive demonstrations have been provided, but practical systems for such applications have not yet been developed.

In the future it may be possible to use phase conjugation to transmit undistorted images through optical fibers (or the atmosphere), to provide lensless imaging down to submicrometer-size resolution to improve optical tracking of objects, phase locking of lasers (although multiple lasers must be close to the same frequency and combining laser beams hasn't yet been shown practical), refreshing of holograms for long-term optical storage, optical interferometry, and image processing. Phase conjugation has demonstrated a number of remarkable phenomena, particularly related to image processing (novelty filtering; edge filtering etc.), but to date only hero demonstrations have been reported. A number of practical issues still must be solved before phase conjugation is likely to be useful. The most likely application lies in telecommunications where it has been shown that nonlinear phase noise is effectively compensated in a midlink optical phase conjugation configuration (Jansen, 2006).

8. Transient nonlinear optics

Some phenomena occur only in the transient regime. These have become particularly important because ultra-short laser pulses (as short as femtoseconds) can provide changes in optical fields faster than any characteristic times in the system. Many of these effects, such as self-induced transparency (Fleischhauer, 2005) and photon echoes (Zewail, 1980; McAuslan, 2011), require quantum mechanical coherence of atomic states and will not be discussed here.

8.1 Self-phase modulation

Self-phase modulation and cross-phase modulation are important transient phenomena that must be included. These phenomena rely on the fact that a pulse traveling through a nonlinear medium sees a time-dependent refractive index, due to the fact that the intensity changes over the time of the pulse. And a time-dependent refractive index introduces a time-variable phase shift that broadens the frequency spectrum of the pulse (Genty, 2007). Because the nonlinear refractive index depends on intensity, when the intensity depends on time through I(t), so does the refractive index, n(t). To first order, its time dependence can be written as $n(t) = n_o + t(\partial n/\partial t) = n_o + tn_2\partial I/\partial t$. A linear variation in time can be considered a frequency shift, so the nonlinear refractive index causing the light to modulate its own phase means that the light undergoes a frequency shift given by $\Delta\nu = n_2(\partial I/\partial t)(z/\lambda_o)$. At

the beginning of a light pulse, the intensity is small, it rises to a maximum and then returns to zero. Thus the phase varies during the duration of the pulse and generates a continuum of frequencies. Pure SPM broadens the frequency spectrum of the pulse symmetrically, introducing a pure phase shift; it does not change the envelope of the pulse in the time domain.

In any real medium, however, dispersion will also act on the pulse. In regions of normal dispersion, the "redder" portions of the pulse have a higher velocity than the "blue" portions, and thus the weaker part of the pulse moves faster than its stronger parts, broadening the pulse in time. In regions of anomalous dispersion, the opposite is true, and the pulse is compressed temporally and becomes shorter. Using femtosecond lasers in specially designed fibers, self-phase modulation can be so large as to produce a white-light continuum which has proven to be very useful for spectroscopy Ranka, 2000).

If the pulse is strong enough, the spectral broadening process of SPM can balance the temporal compression due to anomalous dispersion and reach an equilibrium state, called an optical temporal soliton, discussed later.

Thus we see that self-phase modulation can introduce spectral broadening, extending all the way to a supercontinuum in fiber, or it can compress the pulse in time. When designed properly, self-phase-modulation can also narrow the spectrum (which widens the pulse in time).

8.2 Cross-phase modulation (XPM)

Cross-phase modulation is a direct analog of self-phase modulation in which light at one wavelength can change the phase of light at another wavelength of light through the optical Kerr effect χ_3.

Cross-phase modulation means that different laser pulses within a medium can interact. It is possible to determine the optical intensity of one pulse by monitoring a phase change of the other one. Because no photons in the first beam are absorbed, such a measurement is called quantum nondemolition (QND). XPM can be used to synchronize two mode-locked lasers that co-exist in the same gain medium, as long as the pulses overlap and experience cross-phase modulation. In optical fiber communications, XPM can cause channel cross-talk, particularly in DWDM (dense wavelength division multiplexing) systems. Cross-phase modulation has been considered for wavelength conversion in optical communications, usually based on changes in the refractive index via the carrier density in a semiconductor optical amplifier.

Cross-phase modulation can be used as a technique for adding information to a light stream by modifying the phase of a coherent optical beam with another beam through interactions in an appropriate non-linear medium.

In DWDM applications with intensity modulation and direct detection of several wavelengths transmitted simultaneously, first the signal is phase-modulated by the co-propagating second signal. In a second step dispersion leads to a transformation of the phase modulation into a power variation. The presence of dispersion in this case results in a walk-off of pulses between the channels and reduces the XPM-effect.

8.3 Temporal solitons

A soliton is a wave with a unique shape that travels undisturbed without changing. Solitons require a balance between nonlinearity and dispersion. Optical solitons are most often thought of in the time domain, especially in fibers, where pulse compression due to the optical nonlinearity can overcome the tendency of dispersion to spread pulses out as they travel down a fiber. This happens only for discrete values of the pulse energy and, for positive nonlinearities, the dispersion must be anomalous (negative) (Haus, 1996). Solitons are also called solitary waves and were first discovered in water waves traveling down a canal. Solitons are unique in that they can interact with other solitons and emerge from the collision unchanged, except for a phase shift.

Thus and optical temporal soliton is a pulse of light traveling (usually down a fiber) at its group velocity, while maintaining its same shape. Solitons occur because of an exact balance between dispersion (that tends to spread out the pulse in time) and self-phase-modulation (that tends to widen the spectrum and narrow the pulse). Solitons can be found by solving the non-linear wave equation in the presence of dispersion. The unique time-dependence of the electric field amplitude of the pulse has the form: $E(L,t) = E_o \, \mathrm{sech}(t/T_o)$.

This pulse has a unique amplitude; its peak intensity is linearly proportional to the group velocity dispersion (GVD), $|\partial^2\omega/\partial k^2|$, and inversely proportional to the pulsewidth squared, as shown: $I = n_o \, |\partial^2\omega/\partial k^2| / (\omega_o n_2 v_g^2 T_o^2)$.

Solitons can be explained by considering that the chirp produced by SPM, with high frequencies in back and low frequencies in front, is offset by dispersion, which slows the low frequencies in front of the pulse and speeds the high frequencies in the back of the pulse. The resulting pulse does not change its shape as it travels down the fiber; the dispersion is kept in balance by the nonlinearity and vice versa. If an input pulse does not have the exact soliton shape, a clean soliton will eventually emerge after the undesirable portions of the excitation spread out in time.

Higher order solitary waves exist. An N = 2 soliton starts out as a simple pulse, but as it travels it sharpens in time while developing side-peaks. It fully recovers after a certain period, only to restart the process. The N = 2 soliton requires approximately twice the intensity of the N = 1 soliton. Solitons higher than N = 2 always have multiple peaks in time. These peaks have interesting behaviors, such as passing through each other without interfering. The solutions to the nonlinear wave equation rapidly become very complex and will not be further considered here.

9. Beam-related non-linear effects

To this point we have generally assumed plane waves, either a single wave or interfering waves. (This assumption was violated, however, when describing the Z-scan method for evaluating optical nonlinearities.) A number of interesting phenomena occur when a Gaussian beam, or any other beam of finite width, travels through a nonlinear medium. These effects include self-focusing and optical solitons.

9.1 Self-focusing

When an intense beam is focused into a material with a nonlinear refractive index, the phase velocity decreases with increasing intensity near the center of the beam. This means equiphase

surfaces are compressed near the axis where the beam is more intense. Since rays are normal to the equiphase surfaces, they will tend toward the region of highest intensity, coming to a focus if they can overcome diffraction. This tendency to self-focus is offset by the tendency to diffract. Thus the critical power must be high enough that self-focusing wins.

Self-focusing occurs if the radiation power is greater than a critical power value $P_{cr} = \alpha\lambda^2/(4\pi n_o n_2)$, where λ is the radiation wavelength in vacuum and α is a constant that depends on the initial spatial distribution of the beam and it is approximately 2 for Gaussian-shaped profiles. Of course this critical power depends on the nonlinear coefficient n_2. For air, $n_2 \approx 4\times10^{-23}$ m^2/W for λ = 800 nm, and the critical power is $P_{cr} \approx 2.4$ GW, corresponding to an energy of about 0.3 mJ for a pulse duration of 100 fs. For fused silica, $n_2 \approx 2.4\times10^{-20}$ m^2/W, and the critical power is $P_{cr} \approx 1.6$ MW.

When a beam enters a nonlinear medium, a simple model of a uniform beam of radius a entering a nonlinear medium were $\Delta n = n_2 I$, predicts that it will take a distance z_f before self-focusing occurs, where $z_f{}^2 = (a^2/4)n_o/\Delta n$ (Garmire, 1966). When intense light self-focuses, the intensity becomes large enough that all sorts of additional nonlinearities become large, particularly SRS and SBS. If the beam has hot-spots, the self-focusing action can cause it to break up into filaments (Brewer, 1968). Local areas can become bright enough that they can damage the material. Self-focusing is a real problem that must be overcome in high power nonlinear systems.

9.2 Spatial solitons

The spatial soliton concept preceded self-focusing but is much harder to create in the laboratory. When diffraction and self-focusing are balanced, the nonlinear medium can cause the optical beam to trap itself. As a simple estimate, consider the diffraction of a circular optical beam with a uniform intensity profile in a nonlinear material whose refractive index varies with intensity as $n = n_o + n_2 I$. In a linear medium a beam of diameter D is expected to diffract with angle $\theta_D = 1.22\lambda/n_o D$. For a sufficiently intense beam, the nonlinearity can cause a large enough dielectric discontinuity at the edge of the beam that the critical angle for total internal reflection θ_C is greater than θ_D and the beam cannot diffract. For larger diameter beams, the critical angle θ_C becomes smaller, but so does the diffraction angle θ_D. For smaller diameter beams, θ_C is larger, but so is θ_D. This means there is a particular value of the power, independent of the diameter of the beam, at which we expect to see the beam self-trap. This value is $P_{cr} = 1.22^2\pi\lambda^2/32 n_2 n^2$. (Chiao, 1963, Wright, 1995) The shape must be calculated numerically, but it is clear that the beam area and peak intensity are inversely related, in order to hold the power constant.

For a slab beam there is an analytic solution for the 1D soliton, in which the ideal beam intensity profile is $\mathrm{sech}^2 \Gamma y$, for which there is a critical power, given by $P_{cr} = 2\pi/n_2 n k_o^2$, assuming the nonlinear refractive index is expressed as $n_2 I$. The size of the beam is determined by Γ, which is approximately the inverse beam-width, and is given by $\Gamma = \frac{1}{2}\,\varepsilon_2^{1/2} k_o E_t(0)$, where $E_t(0)$ is the peak value of the optical field.

In a pure χ_3 nonlinearity (optical Kerr effect), the 2D cylindrical beam soliton turns out to be unstable at the critical power, resulting in filamentation and multiple self-focusing. Nonetheless, stable solitons can be created in media with a saturating nonlinearity, or in media with a χ_5 term. In Kerr media, 1D solitons (with a slab beam) are stable. Stable 1D

solitons lasting as long as 5 cm have been reported in carbon disulfide (Barthelemy, 1985). Stable self-trapping can also be observed in the plane of a nonlinear waveguide (Stegeman, 1986). Waveguide confinement out-of-plane means the optical field follows the 2-D solution of the nonlinear wave equation, enabling the beam to travel stably, without diffraction or focusing, in a special in-plane spatial distribution. At higher power, the characteristics of higher-order spatial solitons can be seen (Maneuf, 1988). An amplified mode-locked dye laser with 75 fs pulse-length can to trap itself in a spatial soliton in a glass waveguide 5 mm long (Aitchison, 1990); the small nonlinear coefficient of glass requires high peak power to trap the beam. The guided beam can retain its original 15 μm width at a peak power of $P \sim 400$ kW. While an impressive result, these powers are much too high to be practical.

Spatial optical solitons are possible in a χ_2 medium using the cascading nonlinearity discussed above (Torruellas, 1995). With phase matching, both the fundamental and second harmonic can be mutually trapped.

9.2.1 Spatial solitons in photorefractive media

Spatial solitons can occur in photorefractive media, where the critical power can be on the order of 10 μW (intensities of about 200 mW/cm^2) (Duree, 1993). Photorefractive crystals like SBN have a nonlinearity that can be controlled by a DC applied voltage. Only for a small range of applied voltages is a shape-preserving spatial profile observed to propagate throughout the crystal. These solitons are independent of the light intensity and provide trapping in two dimensions. These are quasi-steady-state solitons, existing only in the time window between the formation of the space-charge grating and the screening of the applied field.

A second kind of photorefractive soliton, called the *screening soliton*, appears in steady state due to the nonuniform screening of the applied field because of nonuniform intensity distribution that can take place in photo-voltaic media (Segev, 1994). A third kind of photo-refractive soliton takes place in lithium niobate, which has a strong photovoltaic current. This results in a photo-voltaic field that changes the refractive index to enable a one-dimensional self-guided spatial soliton (Taya, 1995). The ease with which spatial solitons can now be created has opened up a huge field for experimental study (Stegeman, 1999) with creative new optical profiles (Shu, 2010). Applications are not so readily available, however.

9.2.2 Spark tracks in air

Laser-produced filamentary sparks are the result of instabilities in nonlinear media, particularly in air. The separate regions of ionization suggest that the spatial distribution of the electric field needed for ionization and created by the focused laser beam has regions of maximum and minimum intensities along the beam axis (Berge 2007). Laser-induced breakdown and resulting filaments in air is now a very large field, with work underway to use in weapons.

9.3 Nonlinear waveguides

Waveguides can increase the effective length over which laser light can propagate at high intensity down a nonlinear medium. They can also increase the interaction length between two light waves, enhancing nonlinear phenomena. In addition, there are some particular ways in which the nonlinear refractive index can create or destroy waveguides. Nonlinear

waveguides can exhibit optical bistability (which will be discussed in detail later); this may include thermal nonlinearities as well as the usual χ_3 nonlinearities.

Waveguides increase the effective path length for NLO processes, such as SHG. These processes usually increase quadratically with the interaction length (at least until the process begins to saturate). But the process also depends on the intensity. To achieve high intensity, it is necessary to focus the beam, which usually results in an interaction length only twice the Rayleigh length. Waveguides are the way to overcome this limitation. Waveguides have become important for harmonic generation, because quasi-phase matching is often simpler to create in waveguides than in bulk. Path lengths go from tens of micrometers in a focused beam to several cm, making harmonic generation very practical even for mW lasers.

Highly nonlinear waveguides can be created or destroyed by intense incident light. This is a form of all-optical switching that has been investigated for integrated photonics. Optical creation of waveguides can be seen in bulk photorefractive media, when optical solitons are formed. The nonlinearity may be located in the waveguiding medium itself or in one or more of the media bounding the waveguide.

Within nonlinear waveguides, the shape of the guided mode and its propagation wavevector depend strongly on the optical power. This means incident light power can vary its own coupling efficiency into the waveguide, through the variation of the power-dependent nonlinear refractive index of the spatial layer in the coupling region. In a prism-coupling setup, the optimum coupling angle at high incident power is different from that at low incident power. In end-coupling into a waveguide, the input must have the exact mode shape to achieve (in principle) 100% coupling into the one mode in a single-mode guide. In a nonlinear waveguide, this mode-shape depends on intensity inside the guide. Because coupling into the waveguide depends on the intensity inside the guide, these nonlinear waveguides can exhibit *optical bistability.* By definition, optical bistability means that there are two possible output powers for a single input power. As the input intensity is turned up from zero, the coupling into the waveguide may be poor, because there may be mode mis-match. Thus the output power at a particular power, say P_o, would be some small fraction of the input power. As the input power is turned up toward its maximum, the intensity inside the waveguide may move it toward mode-match, so that a higher fraction of the incident light is coupled into the guide. Thus coupling into the waveguide is now high. Upon lowering the input power back to P_o, the waveguide remains closer to mode-match than it was when the input power was increased to P_o from below. Thus there are two possible output states when the input is P_o. This is an example of optical bistability arising from a non-local nonlinearity. The effective nonlinearity is non-local because the mode-shape arises from the waveguide definition of optimum mode shape. Potential applications lie in the area of all-optical signal processing: bistability, switching, upper and lower threshold devices, optical limiters.

Optical bistability has been observed as a result of opto-thermally-induced refractive index changes. Temperature-induced dispersive OB depends on the temperature change of the real part of the index of refraction affected by a change in the absorption coefficient via the Kramers-Kronig relation. The temperature-dependent change in the optical path length $\Delta(nL)$ is described by a total differential. Neglecting thermal expansion of the sample we have $\Delta(nL)=L\,(\partial n/\partial t)\Delta T$. This kind of nonlinearity requires feedback, forming a kind of NLFP.

Another kind of waveguide bistability utilizes the possibility that the absorption is nonlinear with temperature. Under the right conditions, this leads to a nonlinear equation

that exhibits bistability in output vs. input. Semiconductors present particularly strong example of such bistability (Kim, 1988), as do a number of organic compounds. Polymer dispersed liquid crystals can show thermally induced optical bistability (Mormile, 1998).

Fibers offer an extraordinarily long path length in the χ_3 material fused silica. The ability to make a photonic fibes, with holes along the fiber (a photonic crystal fiber, or PCF) accurate located for specific applications, has made it possible to increase nonlinear effects. PCFs offer single-mode propagation over a broad wavelength range with better mode confinement, increasing the nonlinearity. It is also possible to engineer their group velocity dispersion so as to create phase match. Besides SRS and SBS and FWM, which have been already described in fibers, the phenomena of self-phase modulation and cross-phase modulation occur strongly in these fibers.

Air–silica microstructured optical fibers (sometimes called photonic bandgap crystal fibers) can exhibit anomalous dispersion at visible wavelengths. This provides the phase-matching necessary for a myriad of nonlinear interactions: spectral broadening and continuum generation, stimulated Raman and Brillouin scattering, and parametric amplification. Using photonic crystal fibers and 100 fs pulses, a supercontinuum can be generated, providing a light source from the infrared to the UV (Dudley, 2006). Supercontinuum can be generated using laser pulses as long as several ns or even with high power cw sources. Applications include optical coherence tomography, spectroscopy and optical frequency metrology, leading to the development of a new generation of optical clocks, which has opened up new perspectives to study limits on the drift of fundamental physical constants.

10. Cavity-enhanced nonlinearities

Another way to increase nonlinear effects is to place the nonlinear material in a reflective cavity to resonantly enhance the local optical field. The internal field is increased by the cavity Q. An obvious example is cavity-enhanced SHG. For some nonlinearities, the cavity can provide feedback so that an amplifying process becomes an oscillation. Examples are OPO's and Raman lasers. Finally, some phenomena require a cavity to be observed at all. The nonlinear Fabry-Perot demonstrates optical bistability, for example.

10.1 Resonantly enhanced wave-mixing

Placing a SHG crystal inside the pumping laser resonator has long been a way to increase the SHG efficiency. Internal intensities can be orders of magnitude larger than the external intensity, enabling much larger conversion efficiencies than placing the NLO crystal outside the resonator. The internal intensity $I_{inside} = I_{out}/(1-R)$, where R is the reflectivity of the output mirror, which can be seen by recognizing that (1-R) is the transmission T and $I_{out} = T \bullet I_{inside}$. As an example, today's green laser pointers are frequency-doubled diode-pumped solid-state lasers with a cavity doubling crystal internal to the laser cavity. An alternative is to place the doubling crystal in a cavity *external* to the laser cavity. Conversion efficiencies as high as 75% have been reported with 60 mW cw output (Li 2006) with QPM based on periodic poling.

A cavity can also resonate four-wave mixing, to enhance the output. Examples are photo-refractive films and polymer films.

10.2 Optical Parametric Oscillators (OPOs)

An OPO converts monochromatic laser emission (the *pump*) into a tunable output via a three-wave mixing process. Quantum efficiencies can exceed 50%. The heart of an OPO is a nonlinear-optical (NLO) crystal characterized by an NLO coefficient, $d_{eff,}$ and its related NLO figure of merit, d_{eff}^2/n^3 (where n is the refractive index). In the NLO crystal, the pump photon decays into two less-energetic photons (the signal and the idler) so that the sum of their energies equals that of the pump photon. An important further constraint is that the sum of the signal and idler *wave-vectors* must equal that of the pump ("phase-matching" condition). The latter condition is never satisfied in the transparency range of isotropic media but can be fulfilled in birefringent crystals. Alternatively, it can be fulfilled in quasi-phase-matched (QPM) crystals with periodically modulated nonlinearity (periodically poled lithium niobate, for example) in which the artificially created grating compensates for the wave-vector mismatch.

Parametric frequency down-conversion in an OPO can be regarded as the inverse process of sum-frequency generation. Alternatively, an NLO crystal can be viewed simply as the impetus for the pump photon into break up into two smaller photons. Rotating the crystal changes the ratio between the signal and idler photon energies, and thus tunes the frequency of the output. The easiest way to illustrate parametric frequency conversion is to consider the case of a short (<1 ns) intense pulse as the pump. In this case, a single pass through an NLO crystal is sufficient to convert a substantial fraction of the pump into the signal and the idler. This type of single-pass device is called an optical parametric generator (OPG). For pump pulses with lower intensity, parametric frequency conversion is weaker; therefore, an OPO cavity is required to enhance this process.

The main value in OPOs is that the signal and idler wavelengths, which are determined by phase-matching, can be varied over a wide range. Thus it is possible to produce wavelengths which are difficult or impossible to obtain from any laser (e.g. in the mid-infrared, far-infrared or terahertz regions), with wide wavelength tunability.

10.2.1 Optical parametric oscillator threshold

The threshold for an OPO is calculated by equating the gain of the optical parametric amplifier to the losses in the cavity. The gain can be found by analyzing coupled mode theory for the mixing of the three waves. A strong input pump field E_3 at frequency ω_3 and a weak signal field E_2 at frequency ω_2, which the parametric process will amplify, are incident in a nonlinear medium. The parametric process invokes an idler field at frequency E_1 and frequency ω_1 to complete the interaction, assumed here to be phase-matched: $\mathbf{k}_1 + \mathbf{k}_2 = \mathbf{k}_3$. The coupled mode approach provides three equations:

$$\frac{dE_1(z)}{dz} = i\kappa_1 E_3(z)E_2^*(z) \quad \frac{dE_2(z)}{dz} = i\kappa_2 E_3(z)E_1^*(z) \quad \frac{dE_3(z)}{dz} = i\kappa_3 E_1(z)E_2(z)$$

Assuming no input idler light and no pump depletion, the signal intensity increases with length ℓ as $I_2(\ell) = I_2(0)\sinh^2(\Gamma\ell)$,

where I is the intensity in W/m²; Δk is the phase mismatch; and Γ is the gain factor defined as

$$\Gamma^2 = \frac{8\pi^2 d_{\text{eff}}^2}{c\varepsilon_0 n_1 n_2 n_3 \lambda_1 \lambda_2} I_3(0)$$

Under these assumptions, the signal intensity gain per unit length has a simple form $G_2(\ell) = \sinh^2(\Gamma\ell)$, which for small gains increases quadratically and for large gains increases exponentially as $\exp(2\Gamma\ell)$.

The threshold for the OPO is found by setting the signal gain per unit length equal to its resonator loss per unit length, α, given by $\exp(2\alpha\ell) = R_1R_2$, to obtain $I_{th} = \alpha_2(c\varepsilon_o n_1 n_2 n_3 \lambda_1 \lambda_2)/[8(\pi\ell d_{eff})^2]$. The threshold intensity decreases as the resonator loss decreases (mirror reflectances increase), and quadratically as the length and nonlinearity increase.

10.2.2 OPO applications

OPOs are useful sources for high peak or average power, high conversion efficiency, and broad continuous tunability. They are particularly valuable in the mid-IR (wavelengths >2.5 μm) where there are no tunable lasers similar to Ti:sapphire. New nonlinear-optical materials have enabled compact and efficient OPO's with infrared wavelength tunability far beyond 5 μm, opening up new applications in molecular spectroscopy, atmospheric monitoring, and ultra-sensitive detection. In the 2- to 20-μm portion of the spectrum, gases exhibit uniquely identifiable absorption features. Pollution monitoring, atmospheric chemistry, and chemical and biological warfare detection can benefit from compact and efficient mid-IR laser sources that allow detection of trace gases and vapors by volume, down to the part-per-billion level. Other applications include noninvasive medical diagnosis by breath analysis, ultrasensitive detection of drugs and explosives down to the parts-per-trillion level using cavity ring-down spectroscopy, and short-range terrestrial or near-earth communications.

The OPO is widely used to generate squeezed coherent states and entangled states of light. Considering a single photon in the OPO, each pump photon gives rise to a pair of photons; the signal and idler fields are correlated at the quantum level, which is required for squeezing. The phases of the signal and idler are correlated as well, leading to entanglement, which is a key requirement for quantum computing.

10.3 Nonlinear resonators: Fabry-Perots and rings

When feedback is added to a nonlinear refractive index or absorption interaction, optical switching, optical bistability and multistability can occur, with potential for all-optical logic and computing. While tantalizing for practical applications, the NLFP (nonlinear Fabry-Perot) has rarely seen practicality. In photonics, the NLR (nonlinear ring) may play more of a role. The feedback effect of a cavity can also be artificially created in a hybrid electrical-optical device, which may have their own applications.

Understanding the origin of optical bistability in a NLFP is straight-forward. It was first described using saturable absorption and later it was realized that bistability could be achieved more with a nonlinear refractive index. Suppose a resonator has a characteristic transmission of $T_r = I_{out}/I_{in} = T_r(I_{inside})$, where the last equality defines the functional form of the resonator transmission as a function of the nonlinear absorption or refractive index, which itself depends on intensity. Note the three different values of the intensity: input intensity I_{in}, output intensity I_{out}, and intensity inside the resonator, I_{inside}. What makes the

nonlinear resonator unique is that the light intensity inside the resonator does *not* depend directly on the input light intensity. Instead, the intensity coming *out* of the resonator is proportional to the intensity *inside*. That is, $I_{out} = T_o I_{inside,}$ where T_o is the transmission of the output port of the resonator. In a Fabry-Perot, T_o = 1-R, where R is the reflectivity of the output mirror. Thus the resonator obeys the following: $T_r(I_{out}/T_o) = I_{out}/I_{in.}$. This can be evaluated through plotting $I_{in} = I_{out}/T_r(I_{out}/T_o)$. If the functional form of T_r is multi-valued, such as in a refractive nonlinear Fabry-Perot, whose transmission values repeat modulo 2π, plotting the output vs. the input may demonstrate optical bistability or multi-stability.

Assume a saturable absorption of amount $\Delta\alpha$, lying on a base of unsaturable absorption, with a form given by $\alpha = \alpha_B + \Delta\alpha/(1 + I/I_s)$. It can be shown that to observe bistability it is necessary that $\alpha L/(T + \alpha_B L) > 8$, where T is the transmission of the lossless cavity. Even if $T \rightarrow 0$, bistability still requires that $\Delta\alpha > 7\alpha_B$. Nonlinearities are usually not this large, and so saturable absorption bistability is not usually the predominant form.

Bistability in a NLFP is usually due to a nonlinear refractive index. When the nonlinearity is saturating, it can be shown that if Δn is the maximum refractive index change, then the condition for bistability is $\Delta n k_o L > \alpha L + (1–R_{eff})$, where α is the (unsaturable) loss per unit length inside the cavity and R_{eff} is the average mirror reflectivity (Garmire, 1989). Semiconducting quantum wells have been shown to exhibit optical bistability when placed in a Fabry-Perot (Vivero, 2010), as does porous silicon (Pham, 2011).

Laser diodes also exhibit optical bistability. Many suggestions have been made to make practical all-optical switching devices in semiconductor materials, but to date few practical systems have arisen. One important application for resonating saturable losses has arisen, however. Bragg mirrors with semiconductor saturable absorbers have been shown to be excellent mode-locking devices for femtosecond lasers (Keller, 1996; Khadour, 2010).

The ring resonator is analogous to a Fabry-Perot and therefore exhibits bistability. These resonators are used in optical waveguide circuits and have become more and more practical as technology for micro-circuits has improved. Optical bistability occurs in a 5 μm radius ring resonator fabricated on a highly integrated silicon device. Strong light-confinement makes possible a nonlinear optical response in silicon with pump power of 45 mW, due to a thermal nonlinearity. In such a small device, the thermal speeds can be up to 500 kHz (Almeida, 2004). The ring resonator directionally coupled to a channel waveguide forms a wavelength-sensitive add-drop filter that is very useful in WDM optical communications. The nonlinear ring enables all-optical switching and logic (Parisa, 2009). Photonic crystals can be engineered to replace optical waveguides and provide even more light confinement and even lower switching powers (Yanik, 2003). While still in the realm of research, nonlinear photonic crystal devices are expected to have a bright future in photonics.

10.4 Hybrid optical bistability

Optical bistability can be created by use of electrical feedback, forming a hybrid system. When some fraction of the output of an optical modulator is incident on a photo-detector, its electrical output can be fed back as a change in voltage on the modulator, changing its transmission (Garmire, 1978). This leads to a hybrid bistability that opens up the number of devices that can exhibit optical bistability. One example is the development of devices that might allow parallel interconnects in complex computer systems (Miller, 2000).

11. NLO topics not covered

This section briefly mentions a number of topics in NLO that were not covered in this chapter. Detailed applications of nonlinearities have been skipped, as well as some recent cutting edge research. Theoretical work and modeling has been crucial to the development of NLO, mostly not discussed here. Indeed, inventive ideas, high quality experiments, physically intuitive modeling and deep theoretical understanding have all played their part in creating this exciting field of NLO.

The laser is an exceedingly nonlinear device and, as such, can be used to demonstrate many of the topics discussed in this chapter. Nonlinear gain can be considered an analog to nonlinear absorption; in semiconductor lasers, a change in gain also changes the refractive index. Optical nonlinearities are needed to explain much of the behavior of semiconductor lasers. Mode-locking and Q-switching often use nonlinear media inserted into the laser cavity, and their interaction with the nonlinearities within the laser must be understood. This chapter is limited to passive devices, not including lasers.

This chapter treats mostly stable nonlinear device performance. However, spatial and temporal instabilities can easily arise in nonlinear systems (Cross, 1993), leading to spatial multi-filamentation, as well as self-organization and even chaos. In the time domain, self-pulsing and chaos can also occur, particularly if light is fed back into the nonlinear medium with a time delay (Goldstone, 1983). Such nonlinearities are seen particularly in lasers (Blaaberg, 2007) and nonlinear fibers (Kibler, 2010).

Plasmons are created at the surface between a dielectric and a metal film, due to interaction between propagating light and the metal; interesting phenomena occur if the dielectric medium is nonlinear. Polaritons result from strong coupling between light and an excited electric dipole and can lead to optical nonlinearities. Neither are approached here.

NLO has revolutionized spectroscopy, which now has a vast number of applications, in chemistry, in biology, in environmental studies, etc. For example, nonlinear saturation enables spectroscopists to make measurements inside inhomogeneously broadened lines; multi-photon absorption enables measurement of levels that are symmetry-forbidden in usual one-photon spectroscopy. This chapter touches only on a few examples.

NLO has revolutionized other fields of science. For example, SHG and OPOs provide sources for squeezed light, cooling atoms and molecules to achieve Bose-Einstein condensation, etc. NLO has made ultra-fast optics possible, exploring ultra-fast processes in molecules, solid state materials, chemistry, plasma physics, etc. Nonlinear frequency conversion has enabled ultra-stable frequency sources that have become new, highly-accurate standards, and led to two Nobel prizes. Two-photon fluorescence and Raman lasers are just two examples of techniques that are standard in biomedical research.

The topic categories covered at the 2011 Nonlinear Optics Conference, sponsored by the Optical Society of America give a good idea of the breadth of non-linear optics and what is cutting-edge NLO research. Fundamental studies and new concepts: Quantum optics, computation and communication; single-photon nonlinear optics; Solitons and nonlinear propagation; Ultrafast phenomena and techniques; Surface, interface and nanostructure nonlinearities; Microcavity and microstructure phenomena; High intensity and relativistic nonlinear optics; Slow light; Coherent control; Pattern formation in nonlinear optical

systems. Nonlinear media investigated today are: Atoms, molecules and condensates; Cold atoms; Dielectrics; Semiconductors; Nanostructures; Photonic bandgap structures; Fibers and waveguides; Photorefractives; Nonlinear nanophotonics. Key areas that merge science and applications are: Novel lasers and frequency converters; Micro solid-state photonics. Applications of interest to the NLO community today include: Lasers and amplifiers; Frequency converters and high harmonics generation; Optical communications; Photonic switching; Ultrafast measurement; Nonlinear x-ray optics; Materials processing; Optical storage; Biological elements; Laser induced fusion; Frequency combs and optical clocks.

12. Conclusions

Nonlinear Optics, has been described here in mostly classical terms. Traditional second harmonic generation, sum-frequency and difference-frequency generation, and generation of a DC field take place only in transparent media that lack a center of inversion symmetry and require phase-matching – with an anisotropic crystal or with periodic poling, or other means of quasi-phase matching. Third order nonlinearities do not necessarily require a center of inversion symmetry, nor phase-matching, although these may be required by some processes. These processes may be enhanced by proximity of an atomic or molecular resonance, although these are not required. These NLO processes are described by a dielectric susceptibility that depends on the light's electric field. Closely related are parametric processes, such as the optical parametric oscillator and the optical parametric amplifier. Nonlinear absorption processes may either cause a decrease in a strong absorption line or may increase absorption due to multi-photon processes. Stimulated Raman and Brillouin scattering are laser-like manifestations of well-known low-power phenomena. The former offers an array of new wavelengths, the latter enables phase conjugation.

This review shows how vast the field of nonlinear optics is today and how far it has come since second harmonic generation was demonstrated with a ruby laser in 1961.

13. References

Abeeluck, A.K. & Garmire, E. (2002). Diffraction Response of a Low-Temperature-Grown Photorefractive Multiple Quantum Well Modulator. *Journal of Applied Physics*, Vol. 91, No. 5, March 2002, pp. 2578-2586.

Abolghasem, P., Han, J., Bijlani, B.J., Helmy, A.S. (2010). Type-0 second order nonlinear interaction in monolithic waveguides of isotropic semiconductors. *Optics Express*, Vol. 18, No. 12, Jun 2010, pp. 12681-12689.

Agrawal, G.P. (2010). *Fiber-Optic Communication Systems* (4th ed). Wiley, ISBN: 978-0-470-50511-3, Hoboken, NJ.

Aitchison, J.S., Weiner, A.M., Silberberg, Y., Oliver, M.K., Jackel, J.L., Leaird, D.E., Vogel, E.M. & Smith, P.W.E. (1990). Observation of Spatial Optical Solitons in a Nonlinear Glass Waveguide. *Optics Letters*, Vol. 15, No. 9, May 1990, pp. 471-473.

Almeida, V.R., Lipson, M. (2004). Optical bistability on a silicon chip. *Optics Letters*, Vol. 29, No. 20, Oct 2004, pp. 2387-2389.

Armstrong, J.A., Bloembergen, N., Ducuing, J. & Pershan, P.S. (1962). Interactions between Light Waves in a Nonlinear Dielectric. *Physical Review*, Vol. 127, No. 6, Sept 1962, pp. 1918-1939.

Baehr-Jones, T., Hochberg, M., Wang, G., Lawson, R., Liao, Y., Sullivan, P., Dalton, L., Jen, A., & Scherer, A. (2005). Optical modulation and detection in slotted Silicon waveguides. *Optics Express*, Vol. 13, No. 14, July 2005, pp. 5216-5226.

Bao X., Chen L. (2011). Recent Progress in Brillouin Scattering Based Fiber Sensors, *Sensors*, Vol. 11, No. 4, Apr. 2011, pp. 4152-4187.

Barthelemy, A., Maneuf, S. & Froehly, C. (1985). Propagation Soliton Et Auto-Confinement De Faisceaux Laser Par Non Linearite Optique De Kerr. *Optics Communications*, Vol. 55, No. 3, September 1985, pp. 202-206.

Becerra, F.E., Willis, R.T., Rolston, S.L., Carmichael, H. J., & L. A. Orozco, L.A. (2010). Nondegenerate four-wave mixing in rubidium vapor: Transient regime, *Physical Review A* Vol. 82, Oct 2010, pp. 043833,1-9.

Begley, R.F., Harvey, A.B. & Byer, R.L. (1974). Coherent Anti-Stoke Raman Spectroscopy. *Applied Physics Letters*, Vol. 25, No. 7, Oct 1974, pp. 387-390.

Berge, L., Skupin, S., Nuter, R., Kasparian, J., & Wolf, J.P. (2007). Ultrashort Filaments of Light in Weakly Ionized, Optically Transparent Media. *Reports on Progress in Physics*, Vol. 70, No. 10, Sept 2007, pp. 1633-1713.

Bergmann, K., Theuer, H., & Shore, B.W. (1998). Coherent Population Transfer Among Quantum States of Atoms and Molecules. *Review Modern Physis,* Vol. 70, No. 3, July 1998, pp. 1003-1025.

Blaaberg, S., Petersen, P.M. & Tromborg, B. (2007) Structure, stability, and spectra of lateral modes of a broad-area semiconductor laser, *IEEE Journal Of Quantum Electronics,* Vol. 43, No. 11-12, Nov-Dec 2007, pp. 959-973.

Blanche, P.-A., Bablumian, A., Voorakaranam, R., Christenson, C., Lin, W., Gu, T., Flores, D., Wang, P., Hsieh, W.-Y., Kathaperumal, M., Rachwal, B., Siddiqui, O., Thomas, J., Norwood, R.A., Yamamoto, M. & Peyghambarian, N. (2010). Holographic Three-Dimensional Telepresence using Large-Area Photorefractive Polymer. *Nature*, Vol. 468, Nov 2010, pp. 80–83.

Bloembergen, N. (1967). Stimulated Raman Effect. American Journal of Physics, Vol. 35, No.11, Nov 1967, pp. 989-1023.

Bondani, M. & Andreoni, A. (2002). Holographic Nature of Three-Wave Mixing. *Physical Review A*, Vol. 66, No. 3, Sept 2002, pp. 033805 (1-9).

Bowers, M.W., Boyd, R.W. & Hankla, A.K. (1997). Brillouin-Enhanced Four-Wave-Mixing Vector Phase-Conjugate Mirror with Beam-Combining Capability. *Optics Letters,* Vol. 22, No. 6, March 1997, pp. 360-362.

Brewer, R.G. Lifsitz, J.R. Garmire, E. Chiao, R.Y. & Townes, C.H. (1968). Small-Scale Trapped Filaments in Intense Laser Beams. *Physical Review*, Vol. 166, No. 2, Feb 1968, pp. 326-331.

Broderick, N.G.R., Ross, G.W., Offerhaus, H.L., Richardson, D.J. & Hanna, D.C. (2000). Hexagonally poled lithium niobate: A two-dimensional nonlinear photonic crystal. *Physical Review Letters*, Vol. 84, No. 19, May 2000, pp. 4345-4348.

Byer, R.L. (1997). Quasi-phasematched nonlinear interactions and devices. *Journal of Nonlinear Optical Physics and Materials*, Vol. 6, No. 4, Dec 1997, pp. 549-592.

Chang, T.Y. & Hellwarth, R.W. (1985). Optical-Phase Conjugation by Backscattering in Barium-Titanate. Optics Letters, Vol. 10, No. 8, Aug 1985, pp. 408-410.

Chen, D., Qin, S. & He, S. (2007). Channel-Spacing-Tunable Multi-Wavelength Fiber Ring Laser with Hybrid Raman and Erbium-doped Fiber Gains. *Optics Express*, Vol. 15, No. 3, Feb 2007, pp. 930-935.

Chi, S.H., Hales, J.M., Cozzuol, M., Ochoa, C., Fitzpatrick, M. & Perry, J.W. (2009), Conjugated polymer-fullerene blend with strong optical limiting in the near-infrared, *Optics Express,* Vol. 17, No.24, Dec 2009, pp. 22062-22072.

Chiao, R.Y., Garmire, E. & Townes, C.H. (1964). Self-Trapping of Optical Beams. *Physical Review Letters*, Vol. 13, No. 15, Oct 1964, pps. 479-482.

Cronin-Golomb, M., Fischer, B., White, J.O. & Yariv, A. (1984). Theory and Applications of 4-Wave Mixing In Photorefractive Media. *IEEE Journal of Quantum Electronics*, Vol. 20, No. 1, Jan 1984, pp. 12-30.

Cross M.C. & Hohenberg, P.C. (1993). Pattern-Formation Outside of Equilibrium, *Reviews of Modern Physics,* Vol. 65, No. 3, Jul 1993, pp. 851-1112.

Dainese, P., Russell, P. St. J., Joly, N., Knight, J.C., Wiederhecker, G.S., Fragnito, H.L., Laude, V. & Khelif, A. (2006). Stimulated Brillouin Scattering from Multi-GHz-Guided Acoustic Phonons in Nanostructured Photonic Crystal Fibres. *Nature Physics*, Vol. 2, May 2006, pp. 388-392.

Damzen, M.J., Vlad, V., Mocofanescu, A. & Babin, V. (2003). *Stimulated Brillouin Scattering: Fundamentals and Applications (Series in Optics and Optoelectronics)*. CRC Press, 2003, ISBN 0750308702, Institute of Physics, London.

Dane, C.B., Neuman, W.A. & Hackel, L.A. (1994). High-Energy SBS Pulse-Compression. *IEEE Journal of Quantum Electron*, Vol. 30, No. 8, Aug 1994, pp. 1907-1915.

Demtröder, D. (2008). *Laser Spectroscopy: Vol. 2: Experimental Techniques* (4th ed). ISBN-10: 3540749527, ISBN-13: 978-3540749523, Springer-Verlag, Berlin.

DeSalvo, R., Said, A.A., Hagan, D.J., Van Stryland, E. W., & Sheik-Bahae M. (1996). Infrared to Ultraviolet Measurements of Two-Photon Absorption and n_2 in Wide Bandgap Solids. *IEEE Journal Quantum Electron*, Vol. 32, No. 8, Aug 1996, pp. 1324-1333.

Dohler, G.H. (1986). Doping Superlattices (n-i-p-i Crystals). *IEEE Journal of Quantum Elect*ronics, Vol. 22, No. 9, Sept 1986, pp. 1682-1695.

Dragoman, D. & Dragoman, M. (2004). Terahertz fields and applications. *Progress in Quantum Electronics*, Vol. 28, No. 1, Jan 2004, pp. 1-66.

Dudley, J.M., Genty, G. & Coen, S. (2006). Supercontinuum generation in photonic crystal fiber. Review of Modern Physics, Vol. 78, No. 4, Oct-Dec 2006, pp. 1135-1184.

Duncan, M.D., Mahon, R., Tankersley, L.L. & Reintjes, J. (1988). Transient Stimulated Raman Amplification in Hydrogen. *Journal of the Optical Society of AmericaB-Optical Physics*, Vol. 5, No. 1, Jan 1988 (A) , pp. 37-52.

Duree, G.C., Schultz, J.L., Salamo, G.J., Segev, M., Yariv, A., Crosignani, B., DePorto, P., Sharp, E.J. & Neurgaonkar, R.R. (1993). Observation of Self-Trapping of an Optical Beam due to the Photorefractive Effect. *Physical Review Letters*, Vol. 71, No. 4, July 1993, pp. 533-536.

Eralp, M., Thomas, J., Tay, S., Li, G., Schülzgen, A., Norwood, R.A., Yamamoto, M. & Peyghambarian, N., "Submillisecond response of a photorefractive polymer under single nanosecond pulse exposure," (2006). *Applied Physics Letters,* Vol. 89, No.11, November, 2006 pp. 114105-114107.

Erokhin, A.I. & Smetanin, I.V. (2010). Experimental and Theoretical Study of Self-Phase Modulation in SBS Compression of High-Power Laser Pulses, *Journal of Russian Laser Research*, Vol. 31, No. 5, Sept 2010, pp. 452-461.

Feinberg, J., Heiman, D., Tanguay, A.R. & Hellwarth, R.W. (1980). Photorefractive Effects and Light-Induced Charge Migration in Barium-Titanate. Journal of Applied Physics, Vol. 51, No. 3, March 1980, pp. 1297-1305.

Fiebig, M., Lottermoser, T., Frohlich, D., Goltsev, A.V., & Pisarev, R.V. (2002). Observation of coupled magnetic and electric domains. *Nature*, Vol. 419, No. 6909, Oct 2002, pp. 818-820.

Fiore, A., Berger, V., Rosencher, E., Bravetti, P. & Nagle, J. (1998). Phase matching using an isotropic nonlinear optical material, *Nature*, Vol. 391, Jan 1998, pp. 463-466.

Fleischhauer, M., Imamoglu, A. & Marangos, J.P. (2005). Electromagnetically Induced Transparency: Optics in Coherent Media. *Reviews of Modern Physics*, Vol. 77, No. 2, April 2005, pp. 633 - 673.

Franken, P.A., Hill, A.E., Peters, C.W. & Weinreich, G. (1961). Generation Of Optical Harmonics. *Physical Review Letters,* Vol. 7, No. 4, Aug 1961, pp.118-120.

Fueloep, J.A., Palfalvi L., Hoffmann M.C. & (Hebling, Janos), Towards generation of mJ-level ultrashort THz pulses by optical rectification, *Optics Express* Vol. 19, No. 16, Aug. 2011, pp. 15090-15097.

Garmire, E. (1989). Criteria For Optical Bistability In A Lossy Saturating Fabry-Perot. *IEEE Journal of Quantum Electronics*, Vol. 25, No. 3, Mar 1989, pp. 289-295.

Garmire, E. & Townes, C.H. (1964). Stimulated Brillouin Scattering in Liquids. *Applied Physics Letters*, Vol. 5, No. 4, Aug 1964, pp. 84.

Garmire, E., Chiao, R.Y. & Townes, C.H. (1966) Dynamics and Characteristics of the Self-Trapping of Intense Light Beams. *Physical Review Letters*, Vol. 16, No. 9, Feb 1966, pp. 347-349.

Garmire, E., Jokerst, N.M., Kost, A., Danner, A. & Dapkus, P.D. (1989). Optical Nonlinearities Due to Carrier Transport in Semiconductors. *Journal of the Optical Society of America B-Optical Physics*, Vol. 6, No 4, April 1989, pp. 579-587.

Garmire, E., Marburger, J.H., Allen, S.D. (1978). Incoherent Mirrorless Bistable Optical-Devices. Applied Physics Letters, Vol. 32, No. 5, March 1978, pp. 320-321.

Garmire, E., Townes, C.H. & Pandarese, F. (1963). Coherently Driven Molecular Vibrations and Light Modulation. *Physical Review Letters*, Vol. 11, No. 4, Aug 1963, pp. 160-163.

Geng, J., Staines, S., Wang, A., Zong, J., Blake, M. & Jiang, S. (2006). Highly Stable Low-Noise Brillouin Fiber Laser with Ultranarrow Spectral Linewidth. *IEEE Photonics Technology Letters,* Vol. 18, No. 17, Sept 2006, pp. 1813-1815.

Genty, G., Coen, S., & Dudley, J. M. (2007) Fiber supercontinuum sources (Invited). *Journal of the Optical Society of America B-Optical Physics*, Vol. 24, No. 8, Aug 2007, pp. 1771-1785.

Goldstone, J.A. & Garmire, E.M. (1983). Regenerative Oscillation in the Non-Linear Fabry-Perot-Interferometer. *IEEE Journal of Quantum Electronics*, Vol. 19, No. 2, Feb 1983, pp. 208-217.

Gontier, Y. & Trahin, M. (1968). Multiphoton Ionization of Atomic Hydrogen in Ground State. *Physical Review,* Vol. 172, No. 1, Aug 1968, pp. 83-87.

Grasiuk, A.Z., Kurbasov, S.V. & Losev, L.L. (2004). Picosecond Parametric Raman Laser Based on $KGd(WO_4)_2$ Crystal. *Optics Communications*, Vol. 240, No. 4-6, Oct 2004, pp. 239-244.

Grant-Jacob, J., Mills, B., Butcher, T.J., Chapman, R.T., Brocklesby, W.S. & Frey, J.G. (2011) Gas jet structure influence on high harmonic generation, *Optics Express.* Vol.19, No.10, May 2011, pp.9801-9806

Grazulevicius, J.V., Strohriegl, P., Pielichowski, J. & Pielichowski, A. (2003). Carbazole-containing polymers: synthesis, properties and applications. *Progress in Polymer Science*, Vol. 28, No. 9, Sept 2003, pp. 1297-1353.

Guo, J., Togami, T., Benten, H., Ohkita, H. & Shinzaburo Ito, S. (2009) Simultaneous multi-photon ionization of aromatic molecules in polymer solids with ultrashort pulsed lasers *Chemical Physics Letters*, Vol. 475, No. 4-6, Jun 2009, pp. 240-244.

Gunter, P. (1982). Holography, Coherent Light Amplification and Optical Phase Conjugation with Photorefractive Materials. *Physics Reports (Review Section of Physics Letters),* Vol. 93, No. 4, Dec 1982, pp. 199-299.

Hagley, E.W., Deng, L., Kozuma, M., Wen, J., Helmerson, K.S., Rolston, L. & Phillips, W.D. (1999). A Well-Collimated Quasi-Continuous Atom Laser. *Science*, Vol. 283, No. 5408, March 1999, pp. 1706-1709.

Haus, H.A. & Wong, W.S. (1996). Solitons in Optical Communications. Reviews of Modern Physics, Vol. 68, No. 2, April 1996, pp. 423-444.

Headley, C. & Agrawal, G.P. (Eds.) (2005). *Raman Amplification in Fiber Optical Communication Systems*. Academic Press, ISBN 10: 0-12-044506-9, ISBN 13: 978-0-12-044506-6, Elsevier, Burlington MA.

Heebner, J.E., Bennink, R.S., Boyd, R.W. & Fisher, R.A. (2000). Conversion of Unpolarized Light to Polarized Light with Greater than 50% Efficiency by Photorefractive Two-Beam Coupling. *Optics Letters*, Vol. 25, No. 4, Feb 2000, pp. 257-259.

Hellwarth, R.W. (1977). Third-Order Optical Susceptibilities of Liquids and Solids. *Monographs: Progress in Quantum Electronics*, J.H. Sanders and S. Stenholm, eds., Pergamon Press, New York, 1977, Part I, Vol. 5, pp. 1-68.

Hon, D.T. (1980). Pulse-Compression by Stimulated Brillouin-Scattering. *Optics Letters*, Vol. 5, No. 12, Dec 1980, pp. 516-18.

Horiguchi, T., Shimizu, K., Kurashima, T., Tateda, M., & Koyamada, Y. (1995). Development of a Distributed Sensing Technique Using Brillouin-Scattering. *Journal of Lightwave Technology*, Vol. 13, No. 7, Jul 1995, pp. 1296-1302.

Hsu, C.J., Chiu, K.P., Lue, J.T. & Lo, K.Y. (2011), Enhancement of reflective second harmonic generation using periodically arrayed silver-island films, *Applied Physics Letters*, Vol. 98, No. 26, Jun 2011, pp. 261107,1-3.

Hung, L.J., Diep, L.N., Han, C.C., Lin, C.Y., Rieger, G.W., Young, J.F., Chien, F.S.S. & Hsu, C.C. (2008). Fabrication of spatial modulated second order nonlinear structures and quasi-phase matched second harmonic generation in a poled azo-copolymer planar waveguide, *Optics Express,* Vol. 16, No.11, May. 2008 pp. 7832-7841.

Islam, M.N. (ed.) (2004). *Raman Amplifiers for Telecommunications 1: Physical Principles*. Springer Series in Optical Sciences, Springer-Verlag, ISBN-10: 1441918396, ISBN-13: 978-1441918390, NYC, NY.

Jansen, S.L., van den Borne, D., Spinnler, B., Calabro, S., Suche, H., Krummrich, P.M., Sohler, W., Khoe, G.-D. & de Waardt, H. (2006). Optical phase conjugation for ultra long-haul phase-shift-keyed transmission. *Journal of Lightwave Technology,* Vol. 24, No. 1, Jan. 2006, pp. 54- 64.

Jokerst, N.M. & Garmire E. (1988). Nonlinear Optical-Absorption In Semiconductor Epitaxial Depletion Regions. *Applied Physics Letters*, Vol. 53, No. 10, Sept 1988, pp. 897-899

Kaiser, W. & Garrett, C.G.B. (1961). 2-Photon Excitation in CaF_2 - Eu^{2+}. *Physical Review Letters,* Vol. 7, No. 6, Sept 1961, pp. 229-231.

Kamanina, N.V., Reshak, A.H., Vasilyev, P.Ya., Vangonen, A.I., Studeonov, V.I., Usanov, Yu.E., Ebothe, J., Gondek, E. , Wojcik, W. & Danel A. (2009). "Nonlinear absorption of fullerene- and nanotubes-doped liquid crystal systems", *Physica E*, Vol. 41, No. 1, Jan 2009, pp.391-394.

Keller, U., Weingarten, K.J., Kartner, F.X., Kopf, D., Braun, B., Jung, I.D., Fluck, R., Honninger, C., Matuschek, N. & derAu, J.A. (1996). Semiconductor Saturable Absorber Mirrors (SESAM's) for Femtosecond to Nanosecond Pulse Generation in Solid-State Lasers. *IEEE Journal of Selected Topics in Quantum Electronics*, Vol. 2, No. 3, Sept 1996, pp. 435-453.

Kim, B.G., Garmire, E., Shibata, N., & Zembutsu, S. (1987). Optical Bistability and Nonlinear Switching Due to Increasing Absorption in Single-Crystal Znse Wave-Guides. *Applied Physics Letters*, Vol. 51, No. 7, Aug 1987, pp. 475-477.

Kim, E.J., Yang, H.R., Lee, S.J., Kim, G.Y., Lee, J.W. & Kwak, C.H. (2010) Two beam coupling gain enhancements in porphyrin:Zn-doped nematic liquid crystals by using grating translation technique with an applied dc field, *Optics Communications,* Vol. 283, No. 7, Apr 2010, pp. 1495-1499.

Kirkwood,R.K., Michel, P., London, R. et al. (2011). Multi-beam effects on backscatter and its saturation in experiments with conditions relevant to ignition, *Physics of Plasmas* Vol. 18, May 2011, pp. 056311,1-13.

Khadour, A., Bouchoule, S., Aubin, G., Harmand, J.C., Decobert, J. & Oudar, J.L. (2010). Ultrashort pulse generation from 1.56 μm mode-locked VECSEL at room temperature, *Optics Express* Vol. 18, Sept 2010, pp. 19902-19913.

Kobyakov, A., Kumar, S., Chowdhury, D.Q., Ruffin, A.B., Sauer, M., Bickham, S.R. & Mishra, R. (2005). Design concept for optical fibers with enhanced SBS threshold. *Optics Exp*ress, Vol. 13, No. 14, Jul 2005, pp. 5338-5346.

Kost, A., Garmire, E., Danner, A. & Dapkus, P.D. (1988). Large Optical Nonlinearities in a GaAs/AlGaAs Hetero n-i-p-i Structure. *Applied Physics Letters*, Vol. 52, No. 8, Feb 1988, pp. 637-639.

Kovalev, V.I., Harrison, R.G. & Scott, A.M. (2005). 300 W quasi-continuous-wave diffraction-limited output from a diode-pumped Nd : YAG master oscillator power amplifier with fiber phase-conjugate stimulated Brillouin scattering mirror. *Optics Letters* , Vol. 30, No. 24, Dec 2005, pp. 3386-3388.

Kowalczyk, T.C., Singer, K.D. & Cahill, P.A. (1995). Anomalous-Dispersion Phase-Matched 2nd-Harmonic Generation In A Polymer Wave-Guide. *Optics Letters*, Vol. 20, No. 22, Nov 1005, pp. 2273-2275.

Lenner, M., Rácz, P., Dombi, P., Farkas, G. & Kroó N. (2011). Field enhancement and rectification of surface plasmons detected by scanning tunneling microscopy. *Physical Review B*, Vol. 83, No. 20, May 2011, pp. 205428(1-5).

Lee K.J., Liu S., Gallo K., Petropoulos, P. & Richardson, D.J. (2011) Analysis of acceptable spectral windows of quadratic cascaded nonlinear processes in a periodically poled lithium niobate waveguide, *Optics Express,* Vol. 19, No. 9, Apr. 2011, pp. 8327-8335.

Li, M.J., Demichell, M., He, Q. & Ostrowsky, D.B. (1990). Cerenkov Configuration Second-Harmonic Generation In Proton-Exchanged Lithium-Niobate Guides. *IEEE Journal of Quantum Electronics*, Vol. 26, No. 8, Aug 1990, pp. 1384-1393.

Li, S., Zhang, X., Wang, Q., Zhang, X., Cong, Z., Zhang, H. & Wang, J. (2007). Diode-Side-Pumped Intracavity Frequency-Doubled Nd:YAG/$BaWO_4$ Raman Laser Generating Average Output Power of 3.14 W at 590 nm. *Optics Letters*, Vol. 32, No. 20, Oct 2007, pp. 2951-2953.

Liu, X., Zhang, H., Guo, Y. & Li, Y. (1002). Optimal Design and Applications for Quasi-Phase-Matching Three-Wave Mixing. *IEEE Journal of Quantum Electronics*, Vol. 38, No. 9, Sept 2002, pp. 1225.

Lukin, M.D. (2003). Colloquium: Trapping and manipulating photon states in atomic ensembles. Reviews of Modern Physics, Vol. 75, No. 2, April 2003, pp. 457-472.

Lukin, M.D. (2003). Colloquium: Trapping and manipulating photon states in atomic ensembles. Review of Modern Physics, Vol. 75, No. 2,April 2003, pp. 457-472.

Maker, P.D. & Terhune, R. W. (1965). Study of Optical Effects Due to an Induced Polarization Third Order In Electric Field Strength. Physical Review, Vol. 137, No. 3A, Feb 1965, pp. A801-A818.

Maneuf, S. & Reynaud, F. (1988) Quasi-Steady State Self-Trapping of First, Second and Third Order Subnanosecond Soliton Beams, *Optics Communications*, Vol. 66, No. 5,6, May 1988, pp. 325-328.

Marder, S.R., Kippelen, B., Jen, A.K.Y. & Peyghambarian, N. (1997). Design and Synthesis of Chromophores and Polymers for Electro-optic and Photorefractive Applications. *Nature*, Vol. 388, No. 6645, Aug 1997,pp. 845-851.

Martorell, J., Vilaseca, R. & Corbalan, R. (1997) Second harmonic generation in a photonic crystal. *Applied Physics Letters,* Vol. 70, No. 6, Feb 1997, pp. 702-704.

McCamant, D.W., Kukura, P., Yoon, S. & Mathies, R.A. (2004). Femtosecond Broadband Stimulated Raman Spectroscopy: Apparatus and Methods. *Review Scientific Instruments,* Vol. 75, No. 11, Nov 2004, pp. 4971-4980.

McAuslan D. L.; Ledingham P. M.; Naylor W. R.; Beavan, SE; Hedges, MP., Sellars, MJ & Longdell, J.J. (2011) Photon-echo quantum memories in inhomogeneously broadened two-level atoms, *Physical Review A*, Vol. 84, No. 2, Aug 2011, pp. 022309.

Miller, D.A.B. (2000). Optical Interconnects to Silicon. *IEEE Journal of Selected Topics in Quantum Electronics*, Vol. 6, No. 6, Nov-Dec 2000, pp. 1312-1317.

Mitchell, S.A. (2009). Indole Adsorption to a Lipid Monolayer Studied by Optical Second Harmonic Generation, *Journal of Physical Chemistry B*, Vol. 113, No. 31, Aug 2009, pp. 10693-10707.

Mondia, J.P., van Driel, H.M., Jiang, W., Cowan, A.R., & Young, J.F. (2003). Enhanced second-harmonic generation from planar photonic crystals, *Optics Letters*, Vol. 28 No. 24, Dec 2003, pp. 2500-2502.

Mormile P., Petti L., Abbate M., Musto, P., Ragosta, G. & Villano, P. (1998). Temperature switch and thermally induced optical bistability in a PDLC, *Optics Communications*, Vol. 147, No. 4-6, Feb 1998, pp. 269-273.

Mourou, G.A., Tajima, T. & Bulanov, S.V. (2006). Optics in the relativistic regime. *Review Modern Physics,* Vol. 78, April-June 2006, pp. 309–371.

Mueller, C.T. & Garmire, E. (1984). Photorefractive effect in $LiNbO_3$ Directional Couplers. *Applied Optics*, Vol. 23, No. 23, Dec 1984, pp. 4348-4351.

Nolte, D.D. (1999). Semi-insulating semiconductor heterostructures: Optoelectronic Properties and Applications, Journal of Applied Physics, Vol. 85, No. 9, May 1999, pp. 6259-6289.

Okada, A., Ishii, K., Mito, K. & Sasaki, K. (1992). Phase-Matched 2nd-Harmonic Generation in Novel Corona Poled Glass Wave-Guides. *Applied Physics Letters*, Vol. 60, No. 23, Jun 1992, pp. 2853-2855.

Ostroverkhova, O., & Moerner, W.E. (2004) "Organic photorefractives: mechanisms, materials, and applications," (2004). *Chemical Reviews,* Vol. 104, No.7, July 2007, pp. 3267–3314.

Parameswaran, K.R., Kurz, J.R., Roussev, R.V. & Fejer, M.M.(2002). Observation of 99% pump depletion in single-pass second-harmonic generation in a periodically poled lithium niobate waveguide, *Optics Letters*, Vol. 27, No. 1, Jan 2002, pp. 43-45.

Parisa, A. & Nosrat, G. (2009) All-optical ultracompact photonic crystal AND gate based on nonlinear ring resonators, *Journal of the Optical Society of America B-Optical Physics* Vol. 26, No. 1, Jan 2009, pp. 10-16.

Partovi, A. & Garmire, E.M. (1991). Band-Edge Photorefractivity in Semiconductors - Theory and Experiment. Journal of Applied Physics, Vol. 69, No. 10, May 1991, pp. 6885-6898.

Partovi, A., Garmire, E.M. & Cheng, L.J. (1987). Enhanced Beam Coupling Modulation Using the Polarization Properties of Photorefractive GaAs. *Applied Physics Letters*, Vol. 51, No. 5, Aug 1987, pp. 299-301.

Partovi, A., Millerd, J., Garmire, EM., Ziari, M., Steier, W.H., Trivedi, S.B. & Klein, M.B. (1990). Photorefractivity At 1.5-um in CdTe-V. Applied Physics Letters, Vol. 57, No. 9, Aug 1990, pp. 846-848.

Paschotta, R.(2008) Phase Matching, Encyclopedia for Photoniccs and Laser Technology. http://www.rp-photonics.com/phase_matching.html

Pask, H.M. (2003). The Design and Operation of Solid-State Raman Lasers. *Progress in Quantum Electronics,* Vol. 27, No. 1, 2003, pp. 3-56.

Penner, T.L., Motschmann, H.R., Armstrong N.J., Ezenyilimba, M.C. & Williams, D.J. (1994). Efficient Phase-Matched 2nd-Harmonic Generation Of Blue-Light In An Organic Wave-Guide. *Nature*, Vol. 367, No. 6458, Jan 1994, pp. 49-51.

Pham, A., Qiao, H., Guan, B., Gal, M., Gooding, J.J. &. Reece, P.J. (2011). Optical bistability in mesoporous silicon microcavity resonators, *Journal of Applied Physics* Vol. 109, May 2011, pp. 093113

Preston, S.G., Sanpera, A., Zepf, M., Blyth, W.J., Smith, C.G., Wark, J.S., Key, M.H., Burnett, K., Nakai, M., Neely, D. & Offenberger, A.A. (1996). High-Order Harmonics of 248.6-nm KrF Laser from Helium and Neon Ions. *Physical Review A*, Vol. 53, No. 1, Jan 1996, pp. R31-R34.

Ranka, J.K., Windeler, R.S. & Stentz, A.J. (2000). Visible continuum generation in air-silica microstructure optical fibers with anomalous dispersion at 800 nm. *Optics Letters*, Vol. 25, No. 1, Jan 2000, pp. 25-27.

Scala, M.B., Militello, B., Messina, A. & Vitanov, N.V. (2011). Stimulated Raman adiabatic passage in a system in the presence of quantum noise, *Physical Review A* Vol. 83, Jan 2011, 012101, 1-8.

Segev, M., Valley, G.C., Crosignani, B., DePorto, P. & Yariv, A. (1994). Steady-State Spatial Screening Solitons in Photorefractive Materials with External Applied-Field. *Physical Review Letters* Vol. 73, No. 24, Dec 1994, pp. 3211-3214.

Service, R.F. (2005). New Generation of Minute Lasers Steps into the Light. *Science,* Vol. 307, No. 5715, March 2005, pp. 1551-1552.

Sheik-bahae, M., Said, A.A., Wei, T-H., Hagand, D.J., Van. Stryland, E.W. (1990). Sensitive Measurement of Optical Nonlinearities Using a Single Beam *IEEE Journal of Quantum Electronics,* Vol. 26, No. 4, Apr 1990, pp. 760-769.

Shen, Y.R. (1994). Surfaces Probed By Nonlinear Optics. *Surface Science*, Vol. 299, No. 1-3, Jan 1994, pp. 551-562.

Shen, Y.R. & Bloembergen, N. (1965). Theory of Stimulated Brillouin and Raman Scattering. *Physical Review*, Vol. 137, No. 6A, March 1965, pp. A1787-A1805.

Shiraki, K., Ohashi, M. & Tateda, M. (1996). SBS Threshold of a Fiber with a Brillouin Frequency Shift Distribution. *Journal of Lightwave Technology*, Vol. 14, No. 1, Jan 1996, pp. 50–57.

Short, R.W. & Epperlein, E.M. (1992). Thermal Stimulated Brillouin Scattering in Laser-Produced Plasmas. *Physical Review Letters*, Vol. 68, No. 22, June 1992, 3307-3310.

Shu, J., Joyce, L., Fleischer J.W., Siviloglou, G.A. & Christodoulides, D.N. (2010). Diffusion-Trapped Airy Beams in Photorefractive Media, *Physical Review Letters,* Vol. 104, No. 25, Jun 2010, pp. 253904,1-4.

Smith, D. (1977). High-Power Laser Propagation - Thermal Blooming. *Proceedings of the IEEE*, Vol. 65, No. 12, Dec 1977, pp. 1679-1714.

Sohler, W. & Suche, H. (1978). 2nd-Harmonic Generation In Ti-Diffused $LiNbO_3$ Optical-Waveguides With 25-Percent Conversion Efficiency. *Applied Physics Letters*, Vol. 33, No. 6, Aug 1978, pp. 518-520.

Song, X.H., Yang, W.F.. Zeng, Z.N., Li, R.X. & Xu, Z.Z. (2010). Unipolar half-cycle pulse generation in asymmetrical media with a periodic subwavelength structure *Physical Review A,* Vol. 82, No. 5, Nov 2010, pp. 053821, 1-5.

Stegeman, G.I. , Wright, E.M. , Seaton, C.T. , Moloney, J.V. , Shen, T.P. , Maradudin, A.A. & Wallis, R. F. (1986). Nonlinear Slab-Guided Waves in Non-Kerr-Like Media. *IEEE Journal of Quantum Electronics*, QE-22, No. 6, June 1986, pp. 977-983.

Stegeman, G.I. & Segev, M. (1999). Optical Spatial Solitons and their Interactions: Universality and Diversity. *Science*, Vol. 286, No. 5444, Nov 1999, pp. 1518-1523.

Stegeman, G.I., Hagan, D.J. & Torner, L. (1996). Chi((2)) Cascading Phenomena and Their Applications to All-Optical Signal Processing, Mode-Locking, Pulse Compression and Solitons. *Optical and Quantum Electronics*, Vol. 28, No. 12, Dec 1996, pp. 1691-1740.

Steinhausser, B., Brignon, A., Lallier, E., Huignard, J.P. & Georges, P. (2007). High Energy, Single-Mode, Narrow-Linewidth Fiber Laser Source using Stimulated Brillouin Scattering Beam Cleanup. *Optics Express*, Vol. 15, No. 10, May 2007, pp. 6464-6469.

Taya, M., Bashaw, M., Fejer, M.M., Segev, M. & Valley, G.C. (1995). Observation of Dark Photovoltaic Spatial Solitons. *Phys, Review A,* Vol. 52, No. 4, Oct 1995, 3095-3100.

Tien, P.K., Ulrich, R. & Martin, R.J. (1970). Optical Second Harmonic Generation in Form of Coherent Cerenkov Radiation from a Thin-Film Waveguide. *Applied Physics Letters*, Vol. 17, No. 10, Nov 1970, pp. 447-449.

Torres, J., Coquillat, D., Legros, R., Lascaray, J.P., Teppe, F., Scalbert, D., Peyrade, D., Chen, Y., Briot, O., d'Yerville, M.L., Centeno, E., Cassagne, Cassagne, D. & Albert, J.P. (2004). Giant second-harmonic generation in a one-dimensional GaN photonic crystal. *Physical Review B*, Vol. 69, No. 8, Feb 2004, pp. 085105(1-5).

Torruellas, W.E., Wang, Z., Hagan, D.J., VanStryland, E.W., Stegeman, G.I., Tornner, L. & Menyuk, C.R. (1995). Observation of Two-dimensional Spatial Solitary Waves in a Quadratic Medium. *Physical Review Letters*, Vol. 74, No. 25, June 1995, pp. 5039.

Troccoli, M., Belyanin, A., Capasso, F., Cubukcu, E., Sivco, D.L. & Cho, A.Y. (2005). Raman Injection Laser. *Nature*, Vol. 433, No. 7028, Feb 2005, pp. 845-848.

Tutt, L.W. & Boggess, T.F. (1993). A Review of Optical Limiting Mechanisms and Devices Using Organics, Fullerenes, Semiconductors and Other Materials. *Progress in Quantum Electronics,* Vol. 17, No. 4, 1993, pp. 299-338.

Wang, G.Y., Yang, Y. & Garmire, E. (1995). Experimental-Observation Of Efficient Generation Of Femtosecond 2nd-Harmonic Pulses. *Applied Physics Letters*, Vol. 66, No. 25, Jun 1995, pp. 3416-3418.

Wang, R.Z., Guo, K.X., Liu, Z.L., Chen, B. & Zheng, Y.B., (2009). Nonlinear optical rectification in asymmetric coupled quantum wells, *Physics Letters A,* Vol. 373, No. 7, Feb 2009, pp. 795-798.

Wright, E.M., Lawrence, B.L., Torruellas, W. & Stegeman, G. (1995). Stable self-trapping and ring formation in polydiacetylene para-toluene sulfonate. *Optics Letters*, Vol. 20, No. 24, December 15, 1995, pp. 2481-2483.

Xu, C., Zipfel, W., Shear, J.B., Shear, J.B., Williams, R.M. & Webb, W.W. (1996). Multiphoton fluorescence excitation: New spectral windows for biological nonlinear microscopy. *Proceedings of the National Academy of Sciences*, Vol. 93, No. 20, Oct 1996, pp. 10763-10768.

Yang, C.M., Mahgerefteh, D., Garmire, E., Chen, L., Hu, K.Z. & Madhukar, A. (1994). Sweep-Out Times of Electrons and Holes in an InGaAs/GaAs Multiple-Quantum-Well Modulator. *Applied Physics Letters*, Vol. 65, No. 8, Aug 1994, pp. 995-997.

Yanik M.F. & Fan, S. (2003), High contrast all optical bistable switching in photonic crystal micro cavities, *Appl. Phys. Lett.*, vol. 83, no. 14, Jul 2003, pp. 2739–2741.

Yariv, A. (1978). Phase Conjugate Optics and Real-Time Holography. *IEEE Journal of Quantum Electronics,* Vol. 14, No. 9, Sept 1978, pp. 650-660.

Yoo, S.J.B. (1996). Wavelength conversion technologies for WDM network applications. *Journal of Lightwave Technology*, Vol. 14, No. 6, June 1996, pp. 955-966.

Yu, S., Zhang, Y.J., Zhang, H. & Gu, W. (2007). A tunable wavelength-interchanging cross-connect scheme utilizing two periodically poled LiNbO3 waveguides with double-pass configuration, *Optics Communications,* Vol. 272, No. 2, Apr 2007, pp. 480-483.

Zewail, A.H. (1980). Optical Molecular Dephasing - Principles of and Probings by Coherent Laser Spectroscopy. *Accounts of Chemical Research*, Vol. 13, No. 10, Oct 1980, pp. 360-368.

Zhang, Y., Gao, Z.D., Qi, Z., Zhu, S.N. & Ming N.B. (2008). Nonlinear Cerenkov Radiation in Nonlinear Photonic Crystal Waveguides, *Physical Review Letters*, Vol. 100, Apr 2008, pp. 163904,1-4.

Zhang, L., Xu, S.G., Yang, Z. & Cao, S.K. (2011) Photorefractive effect in triphenylamine-based monolithic molecular glasses with low T(g), Materials Chemistry and Physics, Vol. 126 No. 3 Apr 2011, pp. 804-810.

Zipfel, W.R., Williams, R.M., Christie, R., Nikitin, A.Y., Hyman, B.T., & Webb, W.W. (2003). Live tissue intrinsic emission microscopy using multiphoton-excitenative fluorescence and second harmonic generation. *Proceedings of the National Academy of Sciences of The United States of America,* Vol. 100, No. 12, Jun 2003, pp. 7075-7080.

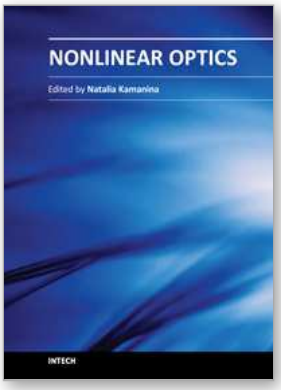

Nonlinear Optics

Edited by Dr. Natalia Kamanina

ISBN 978-953-51-0131-4
Hard cover, 224 pages
Publisher InTech
Published online 29, February, 2012
Published in print edition February, 2012

Rapid development of optoelectronic devices and laser techniques poses an important task of creating and studying, from one side, the structures capable of effectively converting, modulating, and recording optical data in a wide range of radiation energy densities and frequencies, from another side, the new schemes and approaches capable to activate and simulate the modern features. It is well known that nonlinear optical phenomena and nonlinear optical materials have the promising place to resolve these complicated technical tasks. The advanced idea, approach, and information described in this book will be fruitful for the readers to find a sustainable solution in a fundamental study and in the industry approach. The book can be useful for the students, post-graduate students, engineers, researchers and technical officers of optoelectronic universities and companies.

INTECH
open science | open minds

InTech Europe
University Campus STeP Ri
Slavka Krautzeka 83/A
51000 Rijeka, Croatia
Phone: +385 (51) 770 447
Fax: +385 (51) 686 166
www.intechopen.com

InTech China
Unit 405, Office Block, Hotel Equatorial Shanghai
No.65, Yan An Road (West), Shanghai, 200040, China
中国上海市延安西路65号上海国际贵都大饭店办公楼405单元
Phone: +86-21-62489820
Fax: +86-21-62489821